Polybenzimidazole Fuel Cell Technology: Theory, Performance, and Applications

Andrew T. Pingitore[1], Max Molleo[1], Thomas J. Schmidt[2] and Brian C. Benicewicz[1]
[1]Department of Chemistry and Biochemistry, University of South Carolina, University of South Carolina NanoCenter, Columbia, SC, USA
[2]General Energy Research, Laboratory of Electrochemistry, Paul Scherrer Institute, Villigen, Switzerland

Article Outline

Glossary

Combined Heat and Power (CHP): Stationary fuel cell devices that are used to produce both heat and electricity. High temperature PBI fuel cell membranes are well suited for this application.

Conventional Imbibing: The original process of impregnating polymer membranes with dopants. The precast, fully dense membranes are placed in baths of dopants and allowed to absorb the dopant which assists in proton conductivity.

Membrane Electrode Assembly (MEA): A device that is comprised of a PEM that is sandwiched between two electrodes.

Polybenzimidazoles (PBIs): A class of polymers recognized for their excellent thermal and chemical stability, PBIs have historically been spun into fibers and woven into thermal protective clothing. In the past decade, PBIs have been cast into membranes and incorporated into fuel cells.

Polymer Electrolyte Membrane (PEM): Also referred to as Proton Exchange Membranes, PEMs are semi-permeable membranes that conduct and transport protons while preventing the transmission of gases and electrons.

PPA Process: A recently developed imbibing process, PBIs are polymerized and cast in a polyphosphoric acid solvent. Under controlled hydrolysis conditions, Polyphosphoric acid, a good solvent for PBI, is converted into phosphoric acid, a poor solvent for PBI. A mechanically stable PBI gel membrane that is highly doped with phosphoric acid is produced by means of a sol-to-gel transition.

Proton Conductivity: A measure of how well a material can transfer protons. In fuel cell technology, it is used to gauge the viability of proton exchange membranes.

Definition of the Subject

After approximately 15 years of development, polybenzimidazole (PBI) chemistries and the concomitant manufacturing processes have evolved into commercially produced membrane electrode assemblies (MEAs). PBI MEAs can operate reliably without complex water humidification hardware and are able to run at elevated temperatures of 120–180 °C due to the physical and chemical robustness of PBI membranes. These higher temperatures improve the electrode kinetics and conductivity of the MEAs, simplify the water and thermal management of the systems, and significantly increase their tolerance to fuel impurities. Membranes cast by a newly developed polyphosphoric acid (PPA) process possessed excellent mechanical properties, higher phosphoric acid (PA)/PBI ratios, and enhanced proton conductivities as compared to previous methods of membrane preparation. The *p*-PBI and *m*-PBI are

T. E. Lipman, A. Z. Weber (eds.), *Fuel Cells and Hydrogen Production*,
https://doi.org/10.1007/978-1-4939-7789-5_143

Originally published in
R. A. Meyers (ed.), *Encyclopedia of Sustainability Science and Technology*, © Springer Science+Business Media LLC 2018
https://doi.org/10.1007/978-1-4939-2493-6_143-3

the most common polymers in PBI-based fuel cell systems, although AB-PBI and other derivatives have been investigated. This chapter reports on the chemistries and sustainable usages of PBI-based high temperature proton exchange membrane fuel cells (PEMFCs).

Introduction to Polybenzimidazole Fuel Cell Sustainability

Alternative energy is often defined as any energy derived from sources other than fossil fuels or nuclear fission. These alternative energy sources, which include solar, wind, hydro, and geothermal energy, are considered renewable because they are naturally replenished and their supply is seemingly limitless. In contrast, the Earth's supply of fossil fuels is constantly being diminished. Fossil fuels, which include crude oil, coal, and natural gas, continue to be the dominating sources of energy in the world (Fig. 1). Fossil fuels provide more than 86% of the total energy consumed globally [1, 2]. In 2009, the electrical power sector was the largest source of carbon dioxide emissions (40% of all energy-related CO_2 emissions) and was followed closely by the transportation sector which was (34% of the total) [3]. It is predicted that the global demand for fossil fuels will continue to increase over the next 10–20 years due to economic growth. One may conclude that the importance of renewable energy will steadily increase as the Earth's supply of fossil fuels continues to be depleted.

Polymer electrolyte membrane (PEM) fuel cells, also known as proton exchange membrane fuel cells (PEMFCs), are energy conversion devices that could provide the world with clean and efficient energy. Due to their excellent energy production, inexpensive starting materials, and lack of pollutant byproducts, these cells have exponentially gained in popularity over the past decade. Electricity is produced at the heart of the fuel cell by the membrane electrode assembly (MEA), a component that is comprised of a proton exchange membrane sandwiched between two electrodes. Fueled by a hydrogen-based source, a metal catalyst at the anode splits the hydrogen into protons and electrons. As the protons are transported through the proton electrolyte membrane to the cathode, the electrons provide electrical work by traveling around the membrane through an external circuit from the anode to the cathode. The protons and electrons react with an oxidant (typically air or pure oxygen) at the cathode to form water, thereby completing the electrochemical cycle. Hydrogen gas is commonly used as a fuel source for the cells, but other fuels such as methane, methanol, and ethanol have been explored.

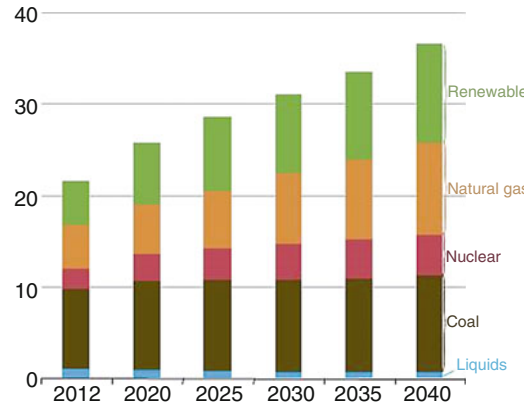

Polybenzimidazole Fuel Cell Technology: Theory, Performance, and Applications, Fig. 1 World net electricity production by source, 2012–2040 (trillion kilowatt hours) [1]

PEM fuel cells provide multiple advantages over conventional fossil fuel energy production. Because water is the only byproduct of the electrochemical process, these fuel cells are clean and environmentally friendly. If one considers the tremendous amount of carbon dioxide created by energy production on the global scale (Fig. 2), PEM fuel cells offer a method to significantly reduce hazardous gas emissions. Minimal moving parts reduces the amount of maintenance of each cell, and the lack of combustion significantly decreases the amount of harmful pollutants such as sulfur oxides and nitrogen oxides. In addition, PEM fuel cells are much more efficient at producing energy (this is discussed in detail in section "PBI/PA Fuel Cell Systems and Their Applications"), and much like a combustion engine, the cell can run continuously as long as

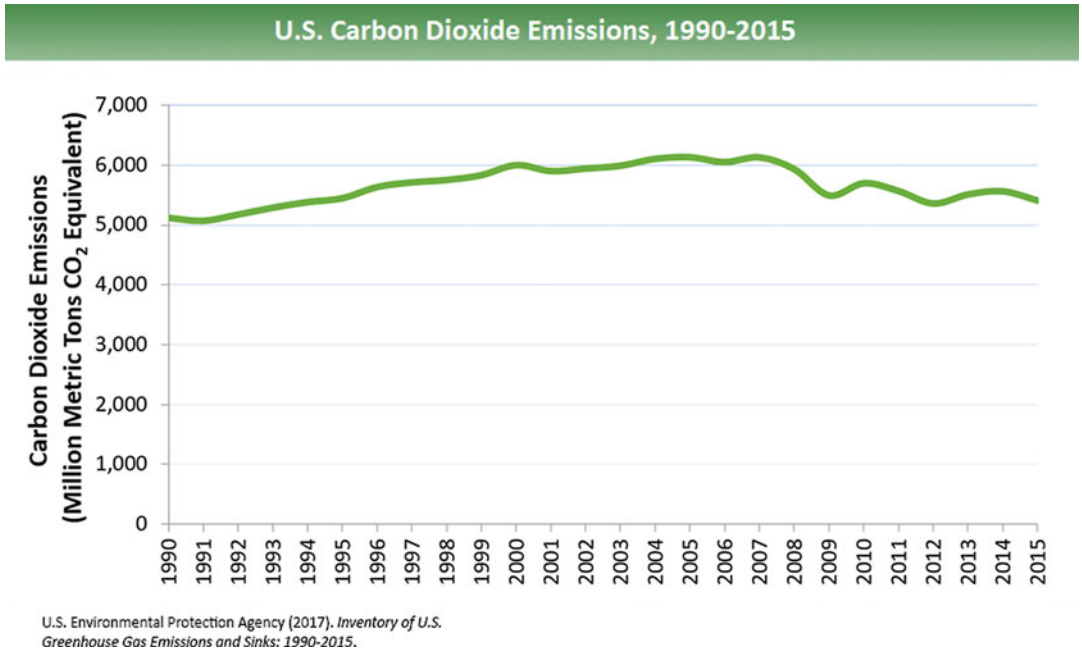

Polybenzimidazole Fuel Cell Technology: Theory, Performance, and Applications, Fig. 2 Global production of carbon dioxide annually from 1990 to 2015 [4]

fuel and oxidant are provided. Although fuel cells are an environmentally friendly energy conversion device, one must consider the way hydrogen is gathered. Both hydrogen production and conversion from chemical to electrical energy need to be sustainable to make the overall process sustainable. Hydrogen production, however, will only briefly be discussed in this chapter.

The efficiency of a PEM fuel cell is largely dependent on the materials used and their arrangement in the cell. Fuel cells use an array of different catalysts, electrodes, membranes, and dopants, each of which function under specific operating conditions. Cells that use low-boiling dopants, such as water, operate at approximately 60–80 °C to avoid vaporization of the proton-transfer agent. Large heat exchangers are required to ensure the heat generated by the cell does not vaporize the electrolyte. Consequently, system complexity is increased as extra components and controls are required to ensure that the membrane remains hydrated during operation. Moreover, cell operation at such low temperatures allows trace amounts of reformate byproducts, especially carbon monoxide, to bind to the catalyst. These highly-competitive, non-reversible reactions "poison" the catalyst, thereby decreasing and possibly terminating the functionality of the fuel cell. Therefore, low temperature fuel cells require an extremely pure fuel source.

In contrast to low-temperature cells, high-temperature PEMs use high-boiling dopants, such as phosphoric acid and sulfuric acid, and function at temperatures of 120–200 °C. Operating at elevated temperatures alleviates the need for excessive heat exchangers and at these temperatures fuel pollutants bind reversibly to the catalyst, which helps to prevent catalyst poisoning. Consequently, high-temperature PEMs can use reformed gases with much higher levels of impurities and lower reformation costs. Furthermore, high temperatures typically improve both the electrode kinetics and operating abilities of the cell. This chapter reports on the chemistries and sustainable usages of PBI-based high temperature PEMFCs.

History and Technical Information of Polybenzimidazole Membranes

Polybenzimidazoles (PBIs) are a class of polymers recognized for their excellent thermal and chemical stability. PBI is used in multiple applications including matrix resins, high strength adhesives, thermal and electrical insulating foams, and thermally resistant fibers. PBI fibers were originally synthesized in the early 1960s by a cooperative effort of the United States Air Force Materials Laboratory with DuPont and the Celanese Research Company. One of the first PBIs to be widely investigated was poly(2,2′-*m*-phenylene-5,5′-bibenzimidazole), which is commonly referred to as *m*-PBI (Fig. 3). Because *m*-PBI is non-flammable, resistant to chemicals, physically stable at high temperatures, and can be spun into fibers, this polymer has been used in astronaut space suits, firefighter's turnout coats and suits, and high temperature protective gloves.

Polybenzimidazole membranes are excellent candidates for high-temperature fuel cells because of their thermal and chemical stability and proton conducting ability. The stability of PBIs is attributed to its aromatic structure (alternating single and double bonds) and the rigid nature of its bonds [5]. While the membrane structure allows protons to flow from one side to the other, it acts as a barrier to the crossover of gases and electrons. The chemical stability of PBIs allows the membranes to withstand the chemically reactive environments of the anode and cathode. Furthermore, the basic nature of the polymer allows it to be highly doped with phosphoric or sulfuric acid. The dopants interact with the polymer matrix and provide a network through which protons can be transported. These acids are used as electrolytes because of their high conductivity, thermal stability, and enhanced proton-transport capabilities. It is important to note that the proton conductivity of PBI membranes without a dopant is negligible. For liquid phosphoric acid, the proton jump rate is orders of magnitude larger than the diffusion of the phosphoric acid molecule as a whole [6]. Additionally, it has been reported that both protons and phosphate moieties have a substantially decreased diffusion coefficient when blended with basic polymers as opposed to liquid phosphoric acid [7]. Therefore, a heterogeneous, two-phase system in which the PBI membrane is phase-separated and imbibed with phosphoric acid has a higher conductivity than its homogeneous counterpart [8]. More recently, Kreuer et al. demonstrated that the interaction of phosphoric acid and PBI reduces the hydrogen bond network frustration, which in turn reduces phosphoric acid's very high acidity and hygroscopicity; reducing electroosmotic drag as well. They suggest this to be a reason why, in fuel cells, PBI-phosphoric acid membranes perform better than other phosphoric acid containing electrolytes with higher protonic conductivity [9]. As evidence of the growing attention in this area, a book on high temperature PEM fuel cells has recently been released [10].

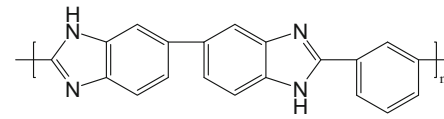

Polybenzimidazole Fuel Cell Technology: Theory, Performance, and Applications, Fig. 3 Chemical structure of poly(2,2′-*m*-phenylene-5,5′-bibenzimidazole) (*m*-PBI)

Synthesis of Polybenzimidazoles

One of the first PBI membranes investigated for fuel cell use was poly(2,2′-*m*-phenylene-5,5′-bibenzimidazole) (*m*-PBI). At the time, there was a vast amount of research previously reported on *m*-PBI and it was renowned for its excellent thermal and mechanical properties [6]. The polymer is synthesized by the reaction of 3,3′,4,4′-tetraaminobiphenyl (TAB) with diphenylisophthalate (DPIP) during a melt/solid polymerization (Scheme 1). The resulting polymer is extracted and has an inherent viscosity (IVs) between 0.5 and 0.8 dL g^{-1}, which corresponds to a polymer with low to moderate molecular weight. The *m*-PBI is further purified by dissolving it in a solution of N, N-dimethylacetamide and lithium chloride (DMAc/LiCl) under 60–100 psi and 250 °C and then filtering; this step removes any crosslinked

m-PBI. The polymer is then cast as a film and dried at 140 °C under vacuum to evaporate the solvent. The *m*-PBI membrane is washed in boiling water to remove any residual DMAc/LiCl solution trapped in the polymer matrix. After the polymer has been dried, an acid bath is used to dope the membrane; the doping level of the membrane can be partially controlled by varying the concentration of acid in the bath. Originally, this conventionally imbibed process created membranes with molar ratios of phosphoric acid/polymer repeat unit (PA/PRU) approximately 6–10 [11]. A "direct acid casting" (DAC) technique was later developed to allow the PBI membrane to retain more PA [12]. Both the conventional imbibing process and DAC were developed following the research performed by Jean-Claude Lasegues, who was one of the first scientists that investigated basic polymeric acid systems (a summary of his work is reviewed in reference [13]). The DAC technique consists of extracting low molecular weight PBI components from PBI powder, and then dissolving the high molecular weight PBI components in trifluoroacetic acid (TFA). Phosphoric acid is added to the TFA/PBI mixture, which is then cast onto glass plates with a casting blade. One may tune the doping level of the polymer by adjusting the amount of phosphoric acid that is added to the TFA/PBI mixture. However, as one increases the PA doping level of a DAC PBI membrane, its mechanical strength decreases to the point where it can no longer be used in a fuel cell. Modern imbibing processes can increase the PA/PBI ratio to 12–16, and these fuel cell membranes are reported to have proton conductivities as high as 0.08 S cm^{-1} at 150 °C at various humidities.

A novel synthetic process for producing high molecular weight PBIs, the "PPA Process" was developed at Rensselaer Polytechnic Institute with cooperation from BASF Fuel Cell GmbH. This process has previously been discussed by Xiao et al. [14] The general synthesis of PBI by this method requires the combination of a tetraamine with a dicarboxylic acid in polyphosphoric acid (PPA) in a dry environment. The step-growth polycondensation reaction typically occurs ca. 200 °C for 16–24 h in a nitrogen atmosphere, producing high molecular weight polymer. This solution is cast directly from PPA as a thin film on a substrate, and upon absorption of water, the PPA hydrolyzes in situ to form phosphoric acid. Note that PPA is a good solvent for PBI while PA is a poor solvent. Under controlled hydrolysis conditions, a mechanically stable PBI gel membrane that is highly doped with phosphoric acid is produced. The multiple physical and chemical transformations that explain the solution-to-gel phase transition are summarized in Fig. 4.

The PA doped *m*-PBI fuel cell membrane maintains thermal and physical stability while operating at high temperature. To illuminate the fundamental differences in polymer film architecture, polymers with similar physical characteristics were prepared by the conventional and PPA Process (Table 1). Even though the ratio of phosphoric acid-to-polymer repeat unit (PA/PRU) achieved by both processes were nearly identical, the PPA Process produces membranes with much higher proton diffusion coefficients and conductivities. One can conclude that the PPA Process creates a membrane with a proton transport architecture superior to that of the conventionally imbibed PBI membrane. The higher proton diffusion coefficients of the membranes produced by the PPA process versus conventionally imbibed membranes were confirmed by NMR [15]. In addition, inherent viscosity data indicates that the PPA Process produces polymers of much higher molecular weight [14]. It was subsequently shown that improved membrane morphology and

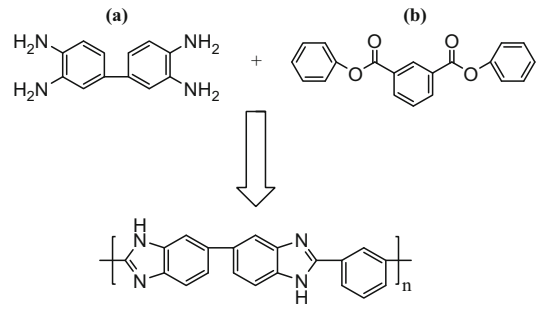

Polybenzimidazole Fuel Cell Technology: Theory, Performance, and Applications, Scheme 1 Polymerization of 3,3′,4,4′-tetraaminobiphenyl (**a**) and diphenylisophthalate (**b**) to form *m*-PBI

increased molecular weight allow the polymer to retain much more phosphoric acid than traditionally cast PBI membranes. An increased PA doping level typically improves the conductivity of the membrane and may even increase the performance of the cell.

Properties and Performance of Synthetically Modified PBI

In this chapter the synthesis of significant PBI membranes (Fig. 5) and their use in fuel cells are described. Synthetically modified PBIs are investigated for enhanced thermo-oxidative stability, solubility, and flexibility; these attributes allow for improved process ability and production of membranes with good chemical and mechanical properties. All PBI membranes are produced by means of step-growth polycondensation reactions and are generally imbibed by either the conventional technique or made by the PPA Process. To synthesize modified polymers, one may either polymerize modified monomers or use post-polymerization crosslinking or substitution reactions. The following sections briefly detail the syntheses of PBI derivatives and their performances as fuel cell membranes.

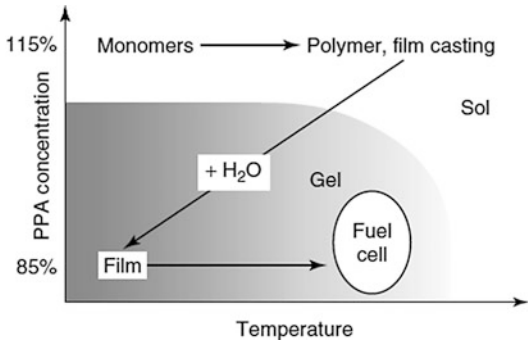

Polybenzimidazole Fuel Cell Technology: Theory, Performance, and Applications, Fig. 4 State diagram of the PPA sol-gel process [14]

m-PBI

One of the first PBI membranes investigated for fuel cell use was *m*-PBI (Fig. 5a). As previously discussed, the film can be processed by using either the conventional imbibing method or the PPA Process. Using the conventional imbibing method, the inherent viscosity of the membrane is usually between 0.50 and 1.00 dL g^{-1} at 30 °C, which indicates polymers of moderate molecular weight. In contrast, *m*-PBI membranes synthesized and doped via the PPA Process have inherent viscosities of approximately 1.00–2.35 dL g^{-1} at 30 °C, which corresponds to higher molecular weight polymers [11]. Using the PPA process, higher molecular weight polymers have contributed to higher doping levels. Phosphoric acid doping levels for conventionally prepared *m*-PBI ranged from 6 to 10 moles PA/PRU, whereas the doping levels for polymer films prepared via the PPA Process range from 14 to 26 moles PA/PRU [5]. Trends show that the mechanical stability of conventionally prepared membranes decrease as the doping level increases and/or as the molecular weight of the polymer decreases. The doping level, casting technique, temperature, and humidity all influence the conductivity of a *m*-PBI membrane. Under various humidities, conventionally prepared *m*-PBI membranes have been reported having conductivities in the range of 0.04–0.08 S

Polybenzimidazole Fuel Cell Technology: Theory, Performance, and Applications, Table 1 Comparison of conventionally imbibed *m*-PBI vs. *m*-PBI synthesized from the PPA process [16]

IV[a] (dl g^{-1})	Film process	Polymer (wt%)	PA (wt %)	Water (wt%)	PA/PBI (molar ratio)	Proton diffusion coefficient[b] (cm^2 s^{-1})	Conductivity[c] (S cm^{-1})
0.89	Conventionally imbibed	15.6	60.7	23.7	12.2	10^{-7}	0.048
1.49	PPA process	14.4	63.3	22.3	13.8	3×10^{-6}	0.13

[a] Inherent viscosity (IV) was measured at a polymer concentration of 0.2 g dl^{-1} in concentrated sulfuric acid (96%) at 30 °C, using a Canon Ubbelohde viscometer
[b] Estimation of upper bound for conventionally imbibed *m*-PBI at 180 °C; PPA-prepared *m*-PBI measured at 180 °C
[c] Measured at 160 °C after an initial heating to 160 °C to remove water

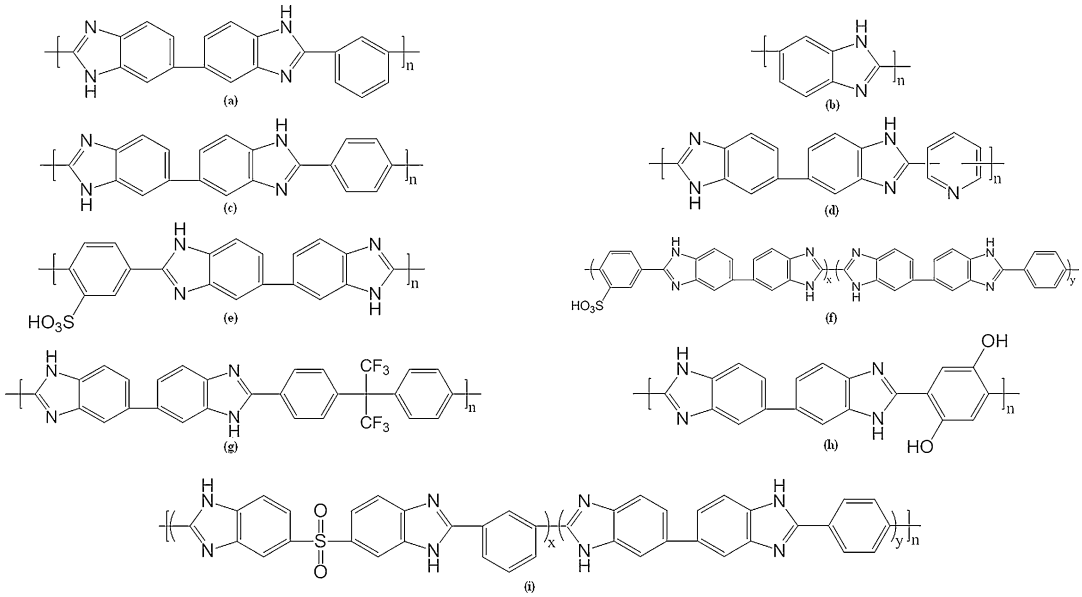

Polybenzimidazole Fuel Cell Technology: Theory, Performance, and Applications, Fig. 5 Various synthetically modified polybenzimidazoles for use in fuel cells. (**a**) *m*-PBI, (**b**) AB-PBI, (**c**) *p*-PBI, (**d**) py-PBI, (**e**) s-PBI, (**f**) s-PBI/*p*-PBI segmented block copolymer, (**g**) 6F-PBI, (**h**) 2OH-PBI, (**i**) *m*-SPBI / *p*-PBI segmented block copolymer

cm^{-1} [17]. Using the PPA Process, the conductivity values of *m*-PBI membranes are typically higher than that of the conventionally imbibed process. One study reported [18] *m*-PBI membranes formed by the PPA process as having a conductivity of 0.13 S cm^{-1} at 160 °C under nonhumidified conditions.

Phosphoric acid doped *m*-PBI membranes that have been formed by the conventional imbibing method have been extensively studied for use in fuel cells. Li et al. [19] demonstrated that a membrane with 6.2 PA/PRU doping level obtains a current density of approximately 0.7 A cm^{-2} at 0.6 V using hydrogen and oxygen gases; these results were promising because the gases were not humidified. Zhai et al. [20] studied the degradation mechanisms of the PA/*m*-PBI system by continuously operating it at 0.640 A cm^{-2} at 150 °C with unhumidified hydrogen and oxygen for 550 h; the fuel cell was operated intermittently the last 50 h with shutoffs every 12 h. The voltage increased from 0.57 to 0.66 V during the beginning 90-h activation period, and the following 450 h period showed a steady decrease to 0.58 V. The performance of the system rapidly decreased in the following 10 h due to agglomeration of the platinum from the catalyst, leaching of the phosphoric acid, and hydrogen crossover. Kongstein et al. [21] employed use of a dual layer electrode to prevent the oxidation of carbon in the polymer membrane, which can occur in acidic environments at high voltages. This electrode would improve the structural integrity of the polymer and help prevent hydrogen crossover from occurring. The PA/*m*-PBI membrane had a maximum of 0.6 V at 0.6 A cm^{-2} with a maximum power density of 0.83 W cm^{-2} at 0.4 V. These performances were lower than that of other PEM systems, such as Nafion, but were still impressive because they could be run at much higher temperatures.

Poly(2,5-polybenzimidazole): AB-PBI

Commonly referred to as AB-PBI, poly(2,5-polybenzimidazole) has a much simpler structure than that of *m*-PBI and other polybenzimidizoles (Fig. 5b). Whereas *m*-PBI is synthesized from

3,3′,4,4′-tetraaminobiphenyl and DPIP, AB-PBI is polymerized from a single monomer, 3,4-diaminobenzoic acid (DABA). This monomer is commercially available and is less expensive than the starting materials of *m*-PBI. The polymer membrane can be cast and imbibed with phosphoric acid by the conventional imbibing method in a mixture of methanesulfonic acid (MSA) and phosphorous pentoxide (P_2O_5) [22] or DMAc. It can also be cast by direct acid casting using trifluoroacetic acid (TFA) [12, 17] or by the PPA Process [12, 23–25] . AB-PBI membranes prepared by the conventional imbibing method had IV values around 2.0–2.5 dL g^{-1} as reported by Asensio et al. [25] and 6–8 dL g^{-1} by Litt et al. [17] Polymers produced from recrystallized DABA by the PPA Process have IV values greater than 10 dL g^{-1} [26]; however, membranes of AB-PBI could not be easily formed via the PPA Process because of the polymer's high solubility in acids.

Because AB-PBI has a high concentration of basic sites (amine and imine groups), it has a high solubility and affinity to acids. Due to this affinity, it can be doped with phosphoric acid and sulfonated with sulfuric acid. Sulfonation of AB-PBI (sAB-PBI) is performed by soaking the precast polymer in sulfuric acid followed by treating the mixture with heat. Asensio et al. [25] reported sAB-PBI/PA membranes having an enhanced conductivity over that of AB-PBI/PA and to be both mechanically strong and thermally stable. Using the direct casting method from MSA-P_2O_5, Kim et al. [22] produced AB-PBI/PA membranes with conductivities similar that of Asensio, having values ranging from 0.02–0.06 S cm^{-1} at 110 °C with no humidification. The conductivity values and physical-chemical properties resemble that of *m*-PBI, making it a good candidate for fuel cell use.

Yu [27] synthesized *p*-PBI-block-AB-PBI membranes to lower the membrane's solubility in acids while maintaining a high acid doping level. Different molar ratios of each polymer block were synthesized, and their conductivities and acid doping levels were investigated. As detailed in Table 2, the proton conductivities of the segmented block copolymers were enhanced by an order of magnitude over that of native AB-PBI. Stress-strain studies showed that these block copolymers were strong enough to be used in fuel cell tests. Polarization curves (Fig. 6) of these membranes illustrate that copolymers II, III, and IV have excellent fuel cell properties (approximately 0.6 V at 0.2 A cm^{-2}); polarization curves for copolymer V and VI could not be measured due to poor thermal stability of the membrane (re-dissolution) at 160 °C.

Poly(2,2′-(1,4-phenylene)5,5′-bibenzimidazole): *p*-PBI

Poly(2,2′-(1,4-phenylene)5,5′-bibenzimidazole) (*p*-PBI, Fig. 5c) is one of the highest performing PBI membranes for high-temperature fuel cell use. Due to the rigid nature of *p*-PBI, high molecular weight polymers have typically been difficult to fabricate or process. The first reported high molecular weight *p*-PBI with an IV value of 4.2 dL g^{-1} was synthesized in 1974 by the United States Air Force Materials Laboratory [28]. Because it could not be spun into fibers as easily as *m*-PBI, *p*-PBI was not investigated further until after the turn of the century. Using the PPA Process, Xiao et al. [16] and Yu et al. [29] synthesized high molecular weight *p*-PBI with IV values as high as 3.8 dL g^{-1}. The PA doping level of the corresponding polymer membranes was >30 mol PA/PRU, allowing the membrane to achieve a conductivity of 0.24 S cm^{-1} at 160 °C. Xiao and Yu showed that *p*-PBI membrane achieves a much higher acid doping level and conductivity than that of *m*-PBI, which only achieves a doping level of 13–16 mol PA/PRU with a conductivity of 0.1–0.13 S cm^{-1}. Because *p*-PBI had excellent mechanical properties at this high doping level, it was a prime candidate for fuel cell performance tests.

The polarization curves of an MEA using *p*-PBI produced by the PPA Process at various temperatures are shown in Fig. 7. Hydrogen was used as the fuel and air was used as the oxidant. The *p*-PBI outperformed the *m*-PBI at all temperatures, and the performance of the MEA increased as the temperature increased. Using a load of 0.2 A cm^{-2}, the cell was able to produce a voltage of 0.606 V at 120 °C; upon raising the temperature

Polybenzimidazole Fuel Cell Technology: Theory, Performance, and Applications, Table 2 Percent composition, acid doping level, and proton conductivity data for various *p*-PBI-block-AB-PBI membranes [27]

	Para-PBI/AB-PBI (mole ratio, x/y)	Acid doping level (PA/2 benzimidazole)	Proton conductivity (S/cm @ 160 °C)	Membrane composition (%)		
				Polymer	H_3PO_4	Water
I	100/0	42.9	0.25	4.13	60.38	35.11
II	75/25	19.1	0.25	8.68	58.09	33.22
III	50/50	24.1	0.27	6.59	54.53	38.88
IV	25/75	21.8	0.23	7.79	63.31	28.90
V	10/90	17.3	0.15	8.84	63.23	27.94
VI	0/100	N/A	N/A			

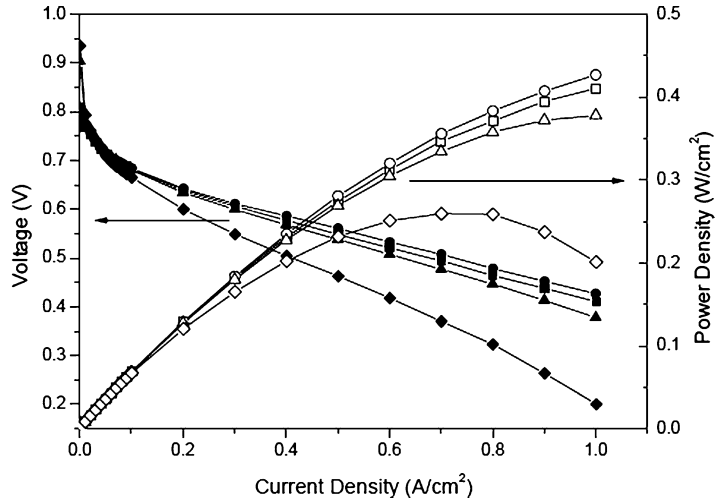

Polybenzimidazole Fuel Cell Technology: Theory, Performance, and Applications, Fig. 6 Polarization curves (*filled symbols*) and power density curves (*unfilled symbols*) of *p*-PBI (Polymer I, ■ □) and *p*-PBI-block-AB-PBI membranes (75/25, Polymer II, ●○, 50/50 Polymer III, ▲Δ, 25/75, Polymer IV, ♦◇) at 160 °C with H_2 (1.2 stoic)/Air (2.0 stoic) under atmospheric pressure [27]

to 180 °C, the voltage increased to 0.663 V. This was especially promising because the gases were unhumidified.

Pyridine-PBI

Pyridine polybenzimidazoles (py-PBIs, Fig. 5d) have been investigated for their use in fuel cells because of their high concentration of basic sites (amine and imine groups). Similar to AB-PBI, the high concentration of basic sites allow these polymers to have a high affinity to acids. The pyridine moiety is commonly combined with the traditional PBI structure by including it as part of the backbone structure.

Xiao et al. synthesized an array of py-PBIs that have the pyridine moiety as part of the polymer backbone [14, 30, 31]. These polymers were synthesized by a reaction of 2,4-, 2,5-, 2,6-, or 3,5-pyridine dicarboxylic acid with 3,3′,4,4′-tetraaminobiphenyl (TAB) using the PPA Process. Exceedingly pure monomers were required to polymerize the py-PBIs, and IV values of 1.0–2.5 dL g^{-1} were obtained. The 2,4- and 2,5-py-PBI membranes formed mechanically strong films, whereas the 2,6-py-PBI membrane was mechanically weak and the 3,5-py-PBI was unable to form films due to high solubility in PPA. All of the py-PBI structures were thermally stable in both nitrogen and air in temperatures up to 420 °C. The 2,5- and 2,6-py-PBI were reported as having conductivities of 0.2 S cm^{-1} and 0.1 S cm^{-1} at 160–200 °C, respectively. The 2,5-py-PBI was found to have the most mechanically robust structure. It was hypothesized that the enhancement of mechanical properties was due to its *para*-orientation as opposed to the other py-PBIs having a *meta*-orientation. In addition, the doping level of

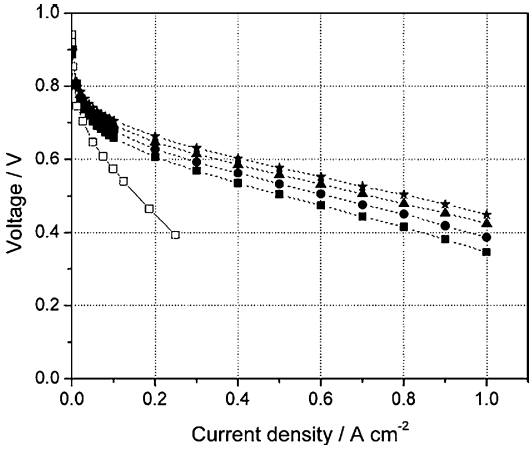

Polybenzimidazole Fuel Cell Technology: Theory, Performance, and Applications, Fig. 7 Polarization curves of PPA-processed *p*-PBI MEA using hydrogen/air at 120 °C (*squares*), 140 °C (*circles*), 160 °C (*triangles*), and 180 °C (*stars*). Open squares represent DMAc cast *m*-PBI MEA at 150 °C [29]

2,5-py-PBI averaged 20 mol of phosphoric acid per polymer repeat unit. Because PPA processed 2,5-py-PBI was an extremely good candidate for fuel cell testing, polarization tests of the MEA were performed (Fig. 8). The platinum loading on the anode and cathode was 1.0 mg cm^{-2} with 30% Pt in Vulcan XC-72 carbon black. The active area for the MEA was 10 cm^2. The membranes used nonhumidified H_2/O_2 and higher temperatures improved the performances of 2,5-py-PBI MEA.

There have been studies indicating that blends of PBI polymers with pyridine-containing polymers could prove useful in a high-temperature PEM fuel cell. Kallitsis et al. [33] combined commercially supplied *m*-PBI with an aromatic polyether that contained a pyridine moiety in the main chain (PPyPO); these polymer blends were then soaked in 85% wt PA. Dynamic mechanical analysis of a 75/25 PBI/PPyPO block copolymer showed reasonable mechanical strength and flexibility. The conductivity of this copolymer was not reported, but the conductivity of 85/15 PBI/PPyPO block copolymer was 0.013 S cm^{-1} at a relatively low PA doping level. Further investigation of these systems is required to prove its utility as a fuel cell membrane.

Sulfonated PBI

Sulfonated aromatic polymers have been widely investigated [34–44] for fuel cell use due to their enhanced physical and chemical robustness, acid and water retention, and conductivity over that of Nafion and other perfluorosulfonic acid-type polymers. Thus, due to the enhanced properties of PBI, it was logical to investigate the physical and chemical properties of sulfonated PBI (s-PBI) membranes. Sulfonation of PBI typically occurs by either direct sulfonation of the polymer backbone [25, 45, 46], grafting sulfonated moieties onto the backbone [25, 47], or by a polycondensation reaction that bonds aromatic tetra-amines to sulfonated aromatic diacids [48–51]. Compared to other sulfonation methods, polycondensation reactions provide more control over the degree of sulfonation.

Mader investigated the physical and chemical properties of s-PBI with PA as the dopant (Fig. 5e) [50]. The polymer was synthesized by two different synthetic pathways; the first was a direct polycondensation reaction of 2-sulfoterephthalic acid (s-TPA) and TAB using the PPA Process, and the second was a postsulfonation reaction of *p*-PBI using concentrated sulfuric acid. The IV values for the polymer membranes derived from the polycondensation reaction ranged from 1 to 2 dL g^{-1}; these polymers had sufficiently high molecular weights to allow strong films to be cast. In addition, these polymer membranes could achieve doping levels between 28 and 53 mol PA/PRU, which resulted in significantly high conductivity values (all above 0.1 S cm^{-1} at all temperatures between 100 °C and 200 °C).

Based on the preliminary data, s-PBI polymer membranes were excellent candidates for fuel cell tests. Polarization tests were run using an s-PBI membrane with an IV value of 1.71 dL g^{-1}, a PA doping level of 52.33 mol PA/PRU, and a conductivity of 0.248 S cm^{-1}; the results are depicted in Fig. 9. The s-PBI membrane exhibited its highest performance at 160 °C, producing 0.6788 V at a current density of 0.2 A cm^{-2}. This performance compares well to that of other PBIs produced by the PPA Process, which is typically around 0.6–0.7 V at 0.2 A cm^{-2}.

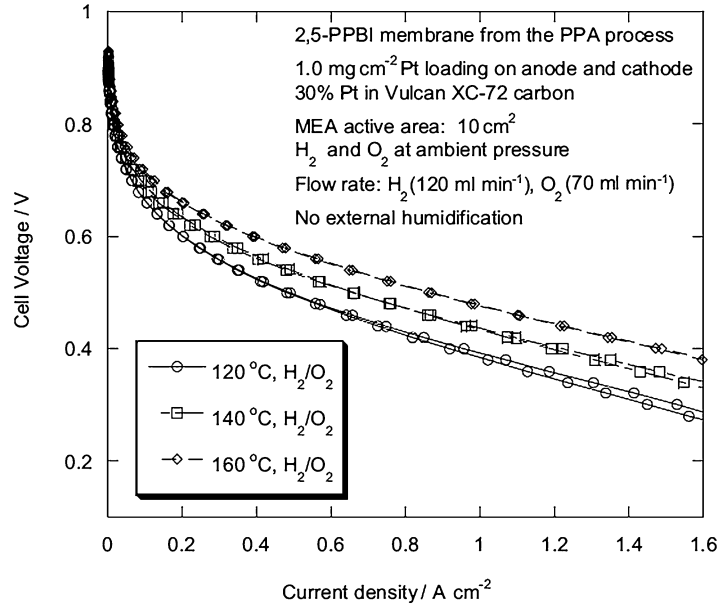

Polybenzimidazole Fuel Cell Technology: Theory, Performance, and Applications,
Fig. 8 Polarization curves under hydrogen and oxygen gases at various temperatures of PA-doped 2,5-py-PBI membranes [32]

The s-PBI homopolymer was shown to have both excellent resistance to gas impurities and excellent longevity. A reformate gas composed of 70% hydrogen, 28% carbon dioxide, and 2% carbon monoxide was used as the fuel while air was used as the oxidant. As depicted in Fig. 10, the fuel cell performance increased with increasing temperature; this is explained by the retardation of carbon monoxide poisoning that occurs at high temperatures. The performance loss of s-PBI MEA was measured by holding the MEA at 0.2 A cm^{-2} at 160 °C for 1200 h using H_2/O_2. After reaching stabilization at the 343rd h, the MEA had a voltage loss of 0.024 mV hr^{-1} for the remainder of the test.

Mader also investigated s-PBI/*p*-PBI random copolymers (Fig. 5f) for use in fuel cells [51]. The random copolymer was synthesized by reacting TAB, TPA, and s-TPA in a reaction flask and the membrane was cast via the PPA Process. High molecular weight polymers were achieved with IV values exceeding 1.8 dL g^{-1}; this allowed for mechanically strong films to be cast. As the ratio of s-PBI/*p*-PBI decreased, the molecular weight of the polymer proportionally increased. Higher PA loading was seen at lower s-PBI/*p*-PBI ratios, which almost directly corresponded to the conductivity of the membranes. The 75/25 s-PBI/*p*-PBI membrane had a PA loading value of 20.32 mol PA/PBI and a conductivity of 0.157 S cm^{-1}, whereas the 25/75 s-PBI/*p*-PBI membrane had a PA loading value of 40.69 mol PA/PBI and a conductivity of 0.291 S cm^{-1}.

Fuel cell performance tests were conducted on the random copolymers. Even though the 25/75 s-PBI/*p*-PBI random copolymer had a higher conductivity than that of p-PBI homopolymer, it was found that all of the random copolymers showed lower performance than *p*-PBI. The 50/50 and 75/25 s-PBI/*p*-PBI random copolymers had lower performance than the s-PBI homopolymer at all PA doping levels. However, the 25/75 s-PBI/*p*-PBI random copolymer performed comparably to the s-PBI homopolymer at equivalent PA doping levels.

PBI-Inorganic Composites

For conventionally prepared PBI membranes, as the acid doping levels of PBIs increase, the conductivity and overall performance of the PBI membranes also tend to increase. However, as high acid doping levels are reached for PBI membranes, the mechanical strength of the membrane significantly decreases. Inorganic fillers for PBI

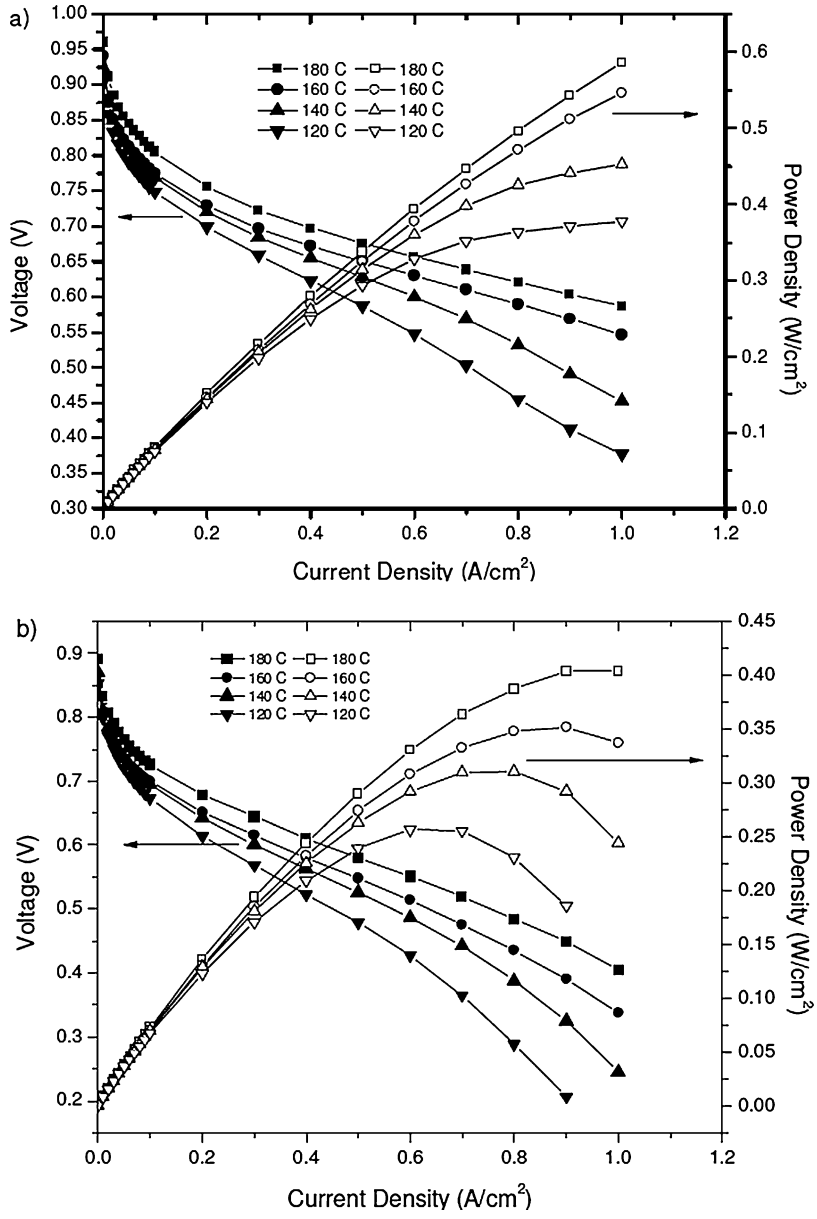

Polybenzimidazole Fuel Cell Technology: Theory, Performance, and Applications,
Fig. 9 Polarization curves (*filled symbols*) and power density curves (*unfilled symbols*) of s-PBI using (**a**) hydrogen and oxygen and (**b**) hydrogen and air [50]

membranes have been investigated to improve membrane film strength, thermal stability, water and acid uptake, and conductivity. These composite membranes have only been examined using *m*-PBI and the conventional casting method.

He et al. investigated the use of zirconium phosphate (ZrP) in a PA/PBI system [52]. The conductivity of *m*-PBI with a doping level of 5.6 PA/PRU increased from 0.068 S cm^{-1} to 0.096 S cm^{-1} with the addition of 15 wt % ZrP at 200 °C and at 5% relative humidity. As seen in Fig. 11, the conductivity of the membrane increased as the relative humidity and temperature of its environment increased. Conductivities of other inorganic fillers, such as phosphotungstic acid, silicotungstic acid, and tricarboxylbutylphosphonate, are comparable or lower than that of ZrP. Unfortunately, there have been no fuel cell performance tests published on these systems. Overall, these inorganic fillers improved the conductivity of *m*-PBI membranes.

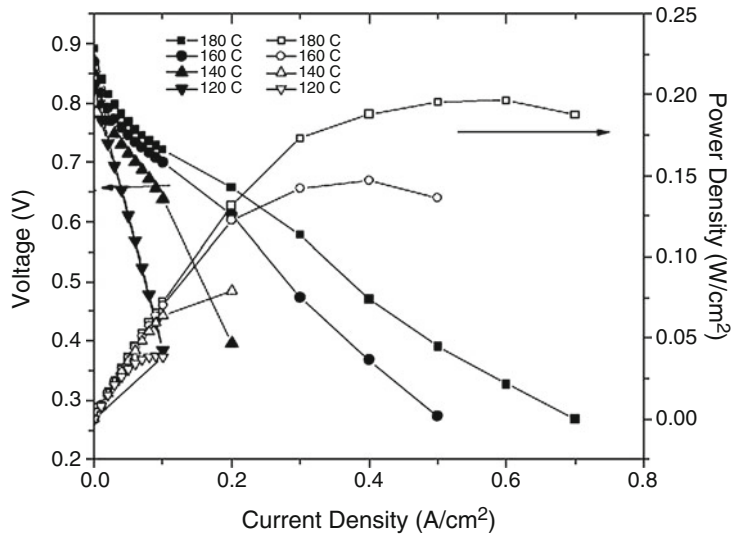

Polybenzimidazole Fuel Cell Technology: Theory, Performance, and Applications,
Fig. 10 Polarization curves (*filled symbols*) and power density curves (*unfilled symbols*) of s-PBI using reformate and air [50]

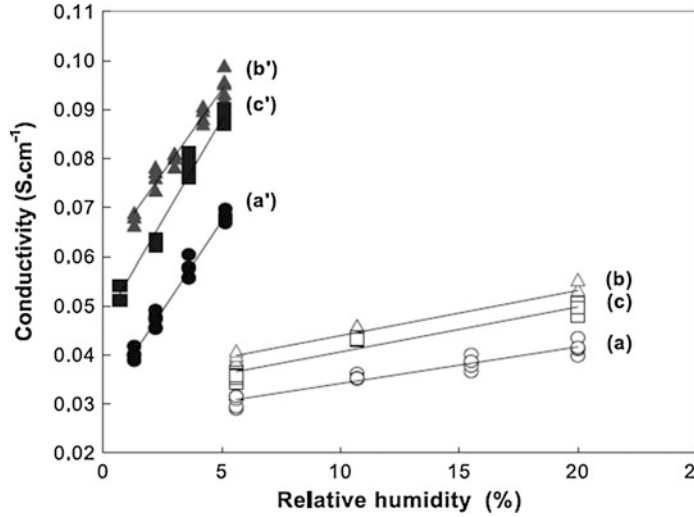

Polybenzimidazole Fuel Cell Technology: Theory, Performance, and Applications,
Fig. 11 Conductivity study of ZrP/*m*-PBI system for (**a**) *m*-PBI at 140 °C, (**a′**) *m*-PBI at 200 °C, (**b**) 15wt% ZrP in *m*-PBI at 140 °C, (**b′**) 15wt% ZrP in *m*-PBI at 200 °C, (**c**) 20wt% ZrP in *m*-PBI at 140 °C, and (**c′**) 20wt% ZrP in *m*-PBI at 200 °C [52]

Other Modified PBIs

Multitudes of other organically modified PBI membranes exist that include, but are not limited to, fluorinated PBI, ionically and covalently crosslinked PBI, PBI blends, and a wide variety of PBI copolymers. Because there are far too many to describe, this subsection will highlight select PBI membranes that have not been included in the prior subsections.

Qian et al. investigated the use of hexafluoroisopropylidene-containing polybenzimidazole (6F-PBI, Fig. 5g) in fuel cell [53]. The polymer was synthesized via the PPA Process through the reaction of TAB with 2,2-Bis (4-carboxyphenyl) hexafluoropropane in PPA. High molecular weight polymer with an IV value of 0.98 dL g^{-1} was achieved. Although the PA doping level of 6F-PBI was considerably high (30–40 mol PA/PRU), the membrane only achieved a peak conductivity value of 0.09 S cm^{-1} at 180 °C. This is lower than that of PPA-processed *p*-PBI that achieved approximately 0.25 S cm^{-1} at 160 °C.

The mechanical strength of 6F-PBI at high PA doping levels was strong enough to fabricate a membrane for fuel cell testing. Polarization and

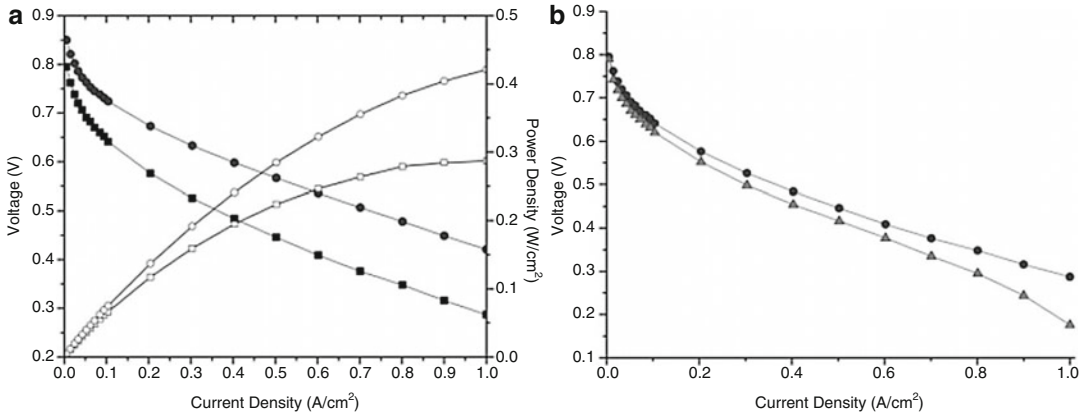

Polybenzimidazole Fuel Cell Technology: Theory, Performance, and Applications, Fig. 12 Graph (**a**) Polarization curves (*filled symbols*) and power density curves (*unfilled symbols*) of 6F-PBI using H_2/Air (*squares*) and H_2/O_2 (*circles*). Graph (**b**) Polarization curves of 6F-PBI using H_2/air (*circles*) and reformate/air (*triangles*) [53]

power density curves of 6F-PBI using hydrogen and reformate gases as fuel are illustrated in Fig. 12. Using hydrogen as fuel and air as the oxidant, the 6F-PBI MEA achieved a steady-state voltage of 0.58 V at a current density of 0.2 A cm^{-2}. When oxygen was used as the oxidant at the same current density, the steady state voltage increased to 0.67 V. Additionally, the MEA showed excellent resistance to carbon monoxide poisoning. When a reformate gas comprised of 40% hydrogen, 40.8% nitrogen, 19% CO_2, and 0.2% CO was used as fuel and air was used as the oxidant, the CO poisoning effects produced an approximate 3 mV reduction in voltage. This study illustrates that low levels of CO poisoning have little effect on the 6F-PBI MEA operating at this temperature.

Commonly known as 2OH-PBI (Fig. 5h), poly (2,2′-(dihydroxy-1,4-phenylene)5,5′-bibenzimidazole) is another PBI membrane with extremely promising properties. Yu and Benicewicz [54] synthesized 2OH-PBI homopolymer by combining TAB with 2,5-dihydroxyterephthalic acid (2OH-TPA) in PPA and cast it via the PPA Process. Yu also synthesized the 2OH-PBI/*p*-PBI random copolymer by reacting both 2OH-TPA and TPA simultaneously with TAB; the copolymer membrane was also cast using the PPA Process. It was proposed that the 2OH-PBI homopolymer was significantly crosslinked through phosphoric acid ester bridges. Because of this crosslinking, the polymer was unable to be dissolved and an IV value could not be determined. Upon hydrolysis of the ester bridges by sodium hydroxide, the IV value of the homopolymer was measured as 0.74 dL g^{-1}. The acid doping level of 2OH-PBI homopolymer was approximately 25 PA/PRU, and its conductivity at 160 °C was 0.35 S cm^{-1}. It is important to note that at all temperatures between room temperature and 180 °C, the conductivity of 2OH-PBI homopolymer was greater than that of *p*-PBI. As the ratio of 2OH-PBI/*p*-PBI decreased in the random copolymer, the doping level and conductivity decreased. It was found that the conductivity of the material was highly dependent on the chemical structure of the PBI membrane and not just the doping level.

Using a Pt anode electrode and a Pt alloy cathode electrode, polarization tests were performed on the homopolymer 2OH-PBI MEA (Fig. 13). The homopolymer produced a voltage of 0.69 V using a load of 0.2 A cm^{-2} at 180 °C and H_2/air; this is greater than the 0.663 V produced by *p*-PBI under the same conditions. The high acid doping level and the membrane chemistry significantly contribute to the excellent performance of the 2OH-PBI membrane. Overall, the fuel cell performance of 2OH-PBI is comparable to that of *p*-PBI.

Segmented PBI block copolymers have also been explored for fuel cell use [55]. Scanlon

synthesized a 52/48 *p*-PBI/*m*-SPBI (Fig. 5i) segmented block copolymer by polymerizing the oligomer of *p*-PBI with that of *m*-SPBI. The oligomers were polymerized in PPA and cast by the PPA Method. Even with an extremely high PA doping level of 91.5 mol PA/PRU, the polymer film had very strong mechanical properties. Under low humidity at 160 °C, the segmented copolymer achieved a conductivity of 0.46 S cm^{-1}. Because of the great results, a *p*-PBI/*m*-SPBI MEA was constructed for use in fuel cell performance tests. The polarization curves of the segmented copolymer MEA displayed a voltage of 0.62 V at 0.2 A cm^{-2} at 160 °C and 0.65 V at 0.2 A cm^{-2} at 200 °C. As implied by the data, these membranes are excellent candidates for high temperature fuel cells.

Membrane Electrode Assembly Durability

As explained in a previous section, a membrane electrode assembly (MEA) consists of the polymer membrane that is sandwiched between an anode and a cathode electrode, respectively. The electrodes are composed of a conductive carbon network that supports a catalyst on a gas diffusion layer. An additive, such as polytetrafluoroethylene (PTFE), helps bind the Pt/C catalyst to the gas diffusion layer. At the anode, the catalyst facilitates the oxidation of hydrogen into its constituent electrons and protons. As the protons are passed through the acid-doped membrane to the cathode, the electrons are passed through an external circuit, thereby creating electricity. Finally, the electrons and protons react with oxygen at the cathode electrode to form water as the final reaction product.

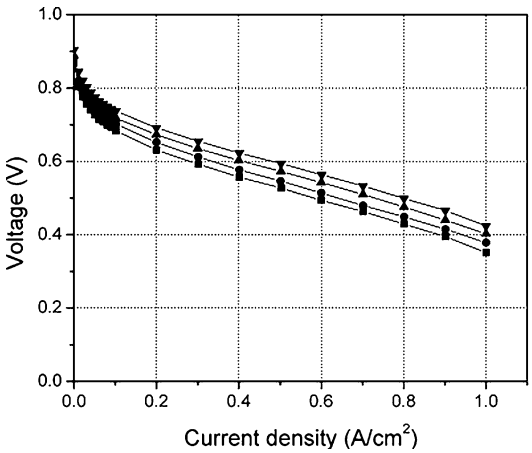

Polybenzimidazole Fuel Cell Technology: Theory, Performance, and Applications, Fig. 13 Polarization curves of 2OH–PBI using hydrogen as the fuel and air as the oxidant at 120 °C (*squares*), 140 °C (*circles*), 160 °C (*triangles*), and 180 °C (*down-triangles*) [54]

Although PBI membranes are highly resistant to degradation, it is possible for the membranes to fail. Common degradation modes for PBI membranes at operating temperatures of 120–200 °C include membrane thinning and pin-hole formation. If there is too much pressure on the membrane, phosphoric acid could be pushed out of the polymer matrix and "thin out" the membrane. An extreme occurrence of membrane thinning results in pin-hole formations. Both of these occurrences result in increased fuel crossover and reduced fuel cell efficiency. Firm gasket materials help to evenly distribute pressure and prevent overcompression of the membrane [56]. Compressive stress of the membrane overtime can also lead to creep, or viscoelastic material flow. Creep and stress relaxation can result in PEM thinning and loss of contact with the electrodes causing degradation in performance.

Chen et al. [57–59] used the compression creep and creep recovery method to study the time-dependent creep behavior of PBI gel membranes. Creep compliance under uniaxial compression offers a direct method to measure viscoelastic deformation under a constant compressive stress. The data was used to directly compare different gel membranes' creep deformation and can then be rationalized in terms of the polymer solids content and polymer composition. Twenty-three different PBI chemistries and 60 different 24 h creep tests were employed to investigate PBI creep behavior. As intuition would suggest, the membranes creep compliance decreased as the polymer solid content increase, when studying the same membrane composition. However, distinct bands of creep compliances were seen across different membrane compositions, see Fig. 14. For example, let us compare *p*-PBI to *m*-PBI. The *p*-PBI is unable to achieve as high a polymer solids content compared to *m*-PBI but has a lower creep compliance. However, in both compositions creep compliance decreases with increasing

polymer solids content. This work uncovered the challenge of finding an optimal compromise between factors that increase polymer solubility in PPA and those that increase sol-gel network strength in PA. This becomes somewhat of a trade-off as the characteristics in which make PBI more soluble in PPA (i.e., increased chain flexibility which promote polymer-solvent interactions) typically decrease the gel network strength.

A potential solution to this problem is designing copolymers containing both a more soluble (flexible) polymer with a more rigid type. This could allow for a higher polymer content while maintaining gel network strength. This was attempted with good results by Benicewicz et al., who looked at multiple different copolymer chemistries. Most notably was the polybenzimidazole 3,5-pyridine-para copolymer made in a 1–5 ratio (83% para and 17% 3,5-pyridine repeat units), Scheme 2.

This copolymer structure allows for the synthesis of a 15% polymer content gel membrane, before preconditioning of the sample, about a 6% increase from the para homopolymer counterpart, with a final post-creep solids content of 31.4%.

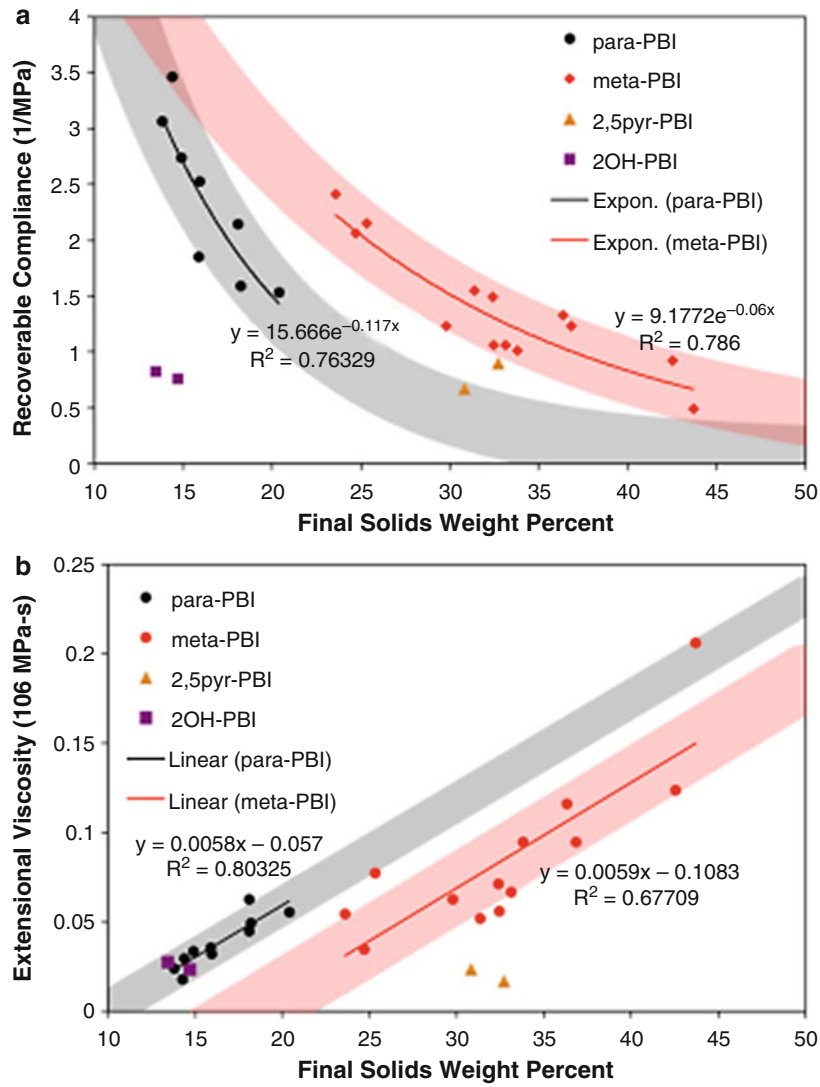

Polybenzimidazole Fuel Cell Technology: Theory, Performance, and Applications,
Fig. 14 Steady-state recoverable compliance J_s^0 (**a**) and extensional viscosity η_0 (**b**) as functions of final solids wt % for para-PBI, meta-PBI, 2,5-pyr-PBI, and 2OH-PBI homopolymers. The solid curves are trend lines fit to the para-PBI and meta-PBI data. The shaded regions are extrapolations of the trend lines, broadened to visually encompass the data points. Each data point is a single compression creep experiment [57]

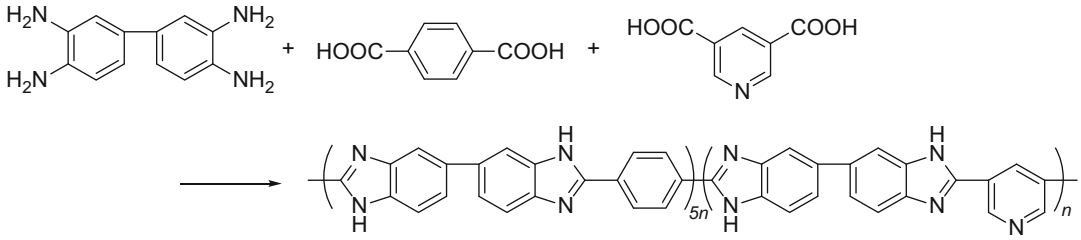

Polybenzimidazole Fuel Cell Technology: Theory, Performance, and Applications, Scheme 2 Synthesis of 3,5-pyridine-para copolymer

The increase in polymer solids due to the copolymer structure demonstrates a creep compliance that falls on the extrapolated para-PBI creep compliance curve, boasting a recoverable compliance (J_s^o) of ~0.6 MPa^{-1}, Fig. 15.

There are other possible avenues to consider when trying to strengthen the polymer network, and those would lie in postmodification techniques. These routes can be employed on both gel and conventionally imbibed PBI membranes. Sondergaard et al. [60] recently published work on enhancing the long-term durability of high temperature PEM fuel cells by thermally cross-linking the PBI membranes. Membranes were fabricated from *m*-PBI by solution casting from *N,N*-dimethylacetamide (DMAc) (a solids content of 10%) on to glass substrates. DMAc was mostly evaporated off by heating the plates to 60 °C for 24 h. The membranes were then thoroughly washed with demineralized water and dried again at 120 °C for an additional 24 h. Following these steps, the membrane underwent a thermal treatment at 350 °C under an argon atmosphere. The now thermally cross-linked membranes were then imbibed with 85% phosphoric acid by soaking in an 85% phosphoric acid bath for 24 h. Long-term fuel cell testing was conducted at 160 °C and a constant current bias of 0.2 A/cm^2 with hydrogen and air flows on the anode and cathode of stoichiometries of 2 and 4, respectively. Long-term data of these fuel cells suggest that the thermal cross-linking increased stability over the nonthermally treated membrane with respect to the voltage degradation. The thermally cured PBI membrane had an average voltage decay rate relative to peak performance of 1.4 μV h^{-1} in contrast to the 4.6 μV h^{-1} of an equivalent cell without a membrane thermal treatment, over a 13,000 h period. It is important to note that shortly after start-up, the fuel cells without the thermally treated membranes showed better performance than the thermally cross-linked, Fig. 16.

The catalyst-coated electrodes of the MEA must be extremely durable in the presence of harsh physical and chemical environments. The oxidation and reduction processes create immense stress on the electrodes and trigger physical and chemical reactions to occur. A summary of the main MEA and component degradation modes have been previously reported [56, 61]. By means of electrochemical Ostwald ripening, Pt-metal agglomeration causes the loss of electrochemical surface area and decrease of reaction kinetics mainly through a dissolution-recrystallization process [62–64]. Oxidation reactions can also cause corrosion of the gas diffusion layer and carbon components in the electrodes, which would result in acid flooding, an increase in mass transport overpotentials, a decrease of reaction kinetics and also, most severely, the loss of the mechanical integrity of the electrodes. Phosphoric acid can dissolve the Pt-metal catalyst and phosphoric acid anions ($H_2PO_4^-$) could adsorb onto the catalyst surface; both of these events would decrease the electrochemical surface area and reaction kinetics. In addition, phosphoric acid evaporation from the catalyst layer would result in similar consequences.

Typical commercial gas diffusion electrodes contain high-surface area carbon supported catalysts, e.g., Pt/Vulcan XC 72. Platinum is

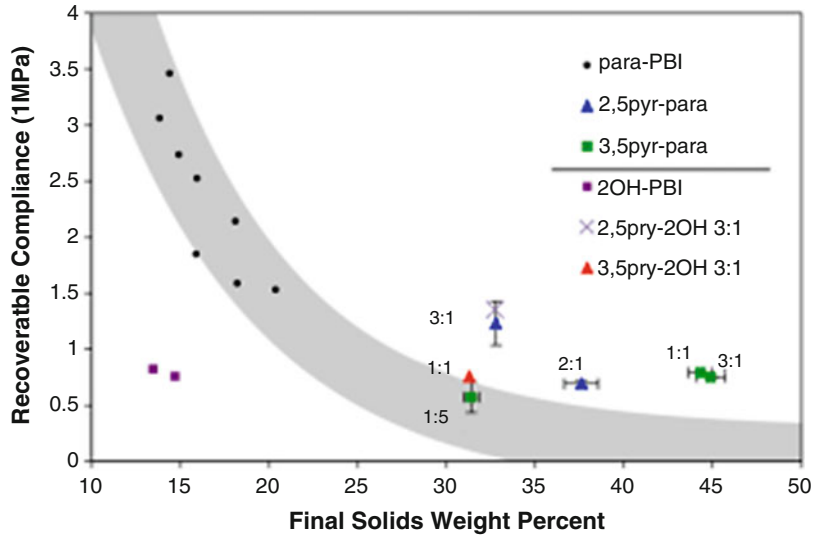

Polybenzimidazole Fuel Cell Technology: Theory, Performance, and Applications, Fig. 15 Steady-state recoverable compliance as a function of final solids wt % for para-PBI and 2OH-PBI homopolymers and related copolymers. For the para-based copolymers, each data point is an average of 2–4 replicate measurements for copolymers with the same copolymer ratio (as indicated in the plot). The data points for the homopolymers and the 2OH-based copolymers are single measurements. The shaded region is the extrapolated trend curve for para-PBI homopolymer [57]

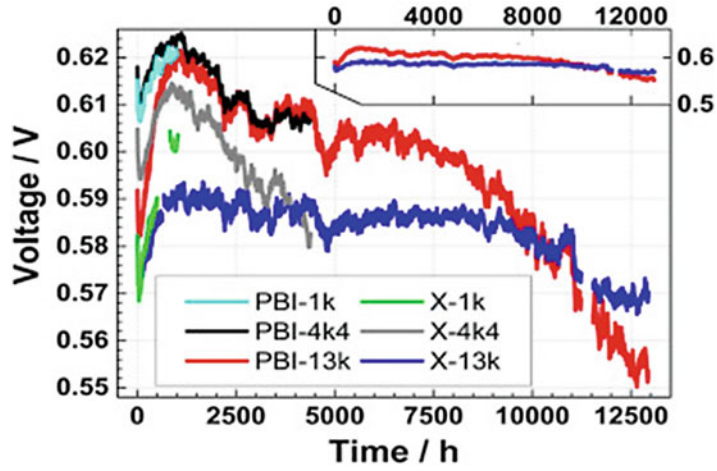

Polybenzimidazole Fuel Cell Technology: Theory, Performance, and Applications, Fig. 16 Steady state lifetime curves for MEAS operated at 160 °C, 200 mA cm^{-2}, stoichiometries of 4 and 2 for air and hydrogen respectively. The insert presents an overview of the two MEA samples that were tested the longest [60]

typically used as the catalyst at both the anode and cathode electrodes because it facilitates the reduction and oxidation reactions at high efficiency. However, due to the degradation modes previously mentioned, performance of the catalyst is lost over time. Novel platinum-based catalysts have been developed to increase the stability of the electrode catalysts. Compared to a commercial Pt/C (46.6 wt.% TKK), Pt_4ZrO_2/C catalysts have been shown to decrease the overall performance loss of the MEA [65]. The Pt_4ZrO_2/C catalyst showed a higher resistance to Pt-sintering than Pt/C following 3000 cycles of a potential sweep test between 0.6 and 1.2 V versus reversible hydrogen electrode (20 mV s^{-1}). The ZrO_2 is thought to act as an anchor to slow the agglomeration of platinum particles.

In order to improve especially the cathode catalyst kinetics and the catalyst stability, alloying of Pt with a base metal such as nickel or cobalt is widely practiced. Origins of these alloys date back to early phosphoric acid fuel cell development [66]. These alloys have been reported to typically improve the cathode kinetics for oxygen reduction by roughly 25–40 mV [66] or a factor of 1.5 to 4 when considering reaction rates. Commercial MEAs using PBI-based membranes also use Pt-base metal alloy catalyst on the cathode [67, 68]. The origin of the kinetic improvements for the Pt-base metal alloys is discussed manifold in the literature [69 –77]: (i) modification of the electronic structure of Pt (5-d) orbital vacancies); (ii) change in the physical structure of Pt (Pt-Pt bond distance and coordination number); (iii) adsorption of oxygen-containing species from the electrolyte onto the Pt or alloying element; and/or (iv) redox-type processes involving the first-row transition alloying elements. However, as discussed in detail in the recent work by Stamenkovic et al. [76], the main effect is a shift of the Pt d-band center to lower energy values which induces a surface which adsorbs oxygenated and spectator species to a lower extent and therefore makes more active sites available for the oxygen reduction to proceed.

Other additives to platinum-based electrodes, such as tin-oxide (SnOx) [78], have also been shown to significantly improve the catalytic activity of the oxygen reduction reaction. Using a PPA processed *m*-PBI membrane with a 7 wt.% SnO in $Pt/SnO_2/C$ catalyst under unhumidified H_2/O_2 at 180 °C, a voltage of 0.58 V under a load of 0.2 A cm^{-2} was produced. Under the same conditions, a *m*-PBI MEA using a Pt/C catalyst produced only 0.4 V at 0.2 A cm^{-2}.

PBI has also been investigated as an additive to platinum-based electrodes. It is thought that incorporation of PBI in the catalyst layer would provide a better interface for proton conduction between the electrode and membrane. Qian [79] incorporated 6F-PBI into the electrodes by four different methods: formation of a PBI bilayer inserting a thin 6F-PBI membrane between an E-TEK cathode and *p*-PBI membrane, casting 6F-PBI/PPA directly onto the E-TEK electrodes and hydrolyzing to form the gel, spraying a 6F-PBI/DMAc solution onto the electrodes, and coating the electrodes with a mixture of 6F-PBI and catalyst (the PBI replaced PTFE). The bilayer method decreased fuel cell performance, and it is proposed that this occurred by creating a large interface resistance between the two PBI layers. Both the casting method and the spraying method improved electrode kinetics, and it is postulated that this occurred due to a lower interface resistance. In addition, a significant decrease in fuel cell performance showed that 6F-PBI could not be used to replace PTFE.

As an outlook to further improvements of catalyst kinetics and durability in low and high temperature polymer electrolyte fuel cells, several possibilities are currently under investigation [80]: (1) extended large scale Pt and Pt-alloy surfaces [76]; (2) extended nanostructured Pt and Pt-alloy films [81]; (3) de-alloyed Pt-alloy nanoparticles [82]; (4) precious metal free catalyst as described by Lefèvre et al. [83], e.g., Fe/N/C catalysts; (5) additives to the electrolyte which modify both adsorption properties of anions and spectator species and also the solubility of oxygen [84]. The latter approach is specific to fuel cells using phosphoric acid as electrolyte.

More recently, catalyst work has been conducted on trying to eliminate the need for expensive platinum. Li et al. [85] have begun work on a platinum-free Fe_3C based oxygen reduction catalyst. They synthesized hollow microsphere morphologies consisting of a graphite layer encapsulated Fe_3C nanoparticles by means of high temperature autoclave pyrolysis. The prepared catalysts demonstrated poor performance compared to traditional platinum based oxygen reduction catalysts; high current densities could not be achieved coupled with low initial voltage output and large voltage decay. Nonetheless, creating a working platinum-free catalyst is notable. More work is still needed in this area if platinum-free catalysts are to become a viable option. An often overlooked area of fuel cell construction is of the flow plates themselves. In 2017 Singdeo et al. [86] modified the conventional serpentine flow field by developing a 5 channel, 6 turn configuration. The conventional flow field,

for some time, has been at the forefront of fuel cell research; however, it displays problematic current density gradients across the cell. At the inlet of the serpentine flow plate the current density has been recorded to be 143% above the mean and 50% below the mean at the outlet; when using 1.3 and 1.4 stoichiometries at the anode and cathode, respectively [84]. This corresponds to a uniformity factor of 0.96. However, with the modified serpentine flow pattern the uniformity factor was increased to 0.998, showing the improved current density distribution. Simulated fuel cell performance testing showed that the new gas flow path improved power output by ~22% at 0.57 V. This work demonstrates that the flow field construction can play a pivotal role in fuel cell performance and further research and experimentation should be considered.

PBI/PA Fuel Cell Systems and Their Applications

Para-PBI is one of the most common polymers used in commercial PBI-based fuel cell systems. A mechanically strong and chemically stable polymer, *p*-PBI has proved to be one of the most reliable PBI polymers for MEA use. Load, thermal, and shutdown-startup cycling tests performed on the *p*-PBI MEA indicated that high temperatures (180 and 190 °C) and high load conditions resulted in slightly increased PA loss from the MEA system. However, steady-state fuel cell operation at 80–160 °C studies showed that PA loss would not be a significant factor in fuel cell degradation [61, 87]. Long-term studies showed minimal performance degradation over a two-year span and indicated excellent commercial fuel cell potential [56]. Compared to state-of-the-art phosphoric acid PEMFCs [88], evaporation of phosphoric acid from commercial PBI-based Celtec P1000 MEAs is reduced by a factor of roughly 2–3. This is a key factor of long-term stable operation for PBI-based fuel cells.

For the transition of PBI-based fuel cell science into commercial products, the appropriate manufacturing processes need to be developed. Most companies rely on manual operations [89] for PBI-based MEA fabrication. Only recently have significant efforts been devoted to developing automated production lines because simple changes in MEA materials and architecture could necessitate the use of different manufacturing equipment. To accommodate the evolution of fuel cell science, a flexible modular manufacturing line has been developed. In 2002, BASF Fuel Cell GmbH (previously PEMEAS) began using the line to accommodate three generations of MEAs. The details of their manufacturing process will be further discussed in section "Advances in PBI MEA Manufacturing." It is important to mention that BASF Fuel Cell GmbH is no longer in existence; however, they are continuing to supply PBI-based MEAs into the commercial market.

Commercial PBI-based high temperature PEMFCs provide energy to a wide array of electronic devices. Hydrogen fuel cell vehicles, both for the private consumer and public transportation, are growing in popularity as pollution and fossil fuel prices continue to increase. Hydrogen offers 2–3 times the overall efficiency in a fuel cell as gasoline does in a typical combustion engine [90]. High temperature fuel cells are also popular as backup generators and combined heat and power devices for stationary use. These types of systems typically produce 1–10 kW, which is enough energy to power a house or a multifamily dwelling. In addition to providing energy, combined heat and power devices use waste heat to heat water and preheat the fuel cell system components, thereby increasing the overall efficiency of the fuel cell system. Fuel cells also offer applications in mobile electronic devices such as laptops and cell phones. Commonly coupled with a methanol reformer, these fuel cell systems are remarkably portable and can power electronics for many hours of continuous use.

In addition to producing electricity, these PEMs have been used as a purification device for hydrogen gas. Consider the purification device to have the same basic architecture as a fuel cell. A platinum catalyst splits contaminated hydrogen gas into protons and electrons at the anode. Using an external power source, the electrons are driven through an external circuit to the cathode while the protons are allowed to transport across the

membrane from the anode to the cathode. The electrons and protons recombine, thereby creating a higher purity hydrogen gas at the cathode while leaving behind the undesired constituents at the anode. These hydrogen pump devices will be further discussed in section "H_2 Pump."

In-Depth Analysis of PPA Processed *p*-PBI MEA

PBI-based high temperature MEAs offer many benefits over more well-known perfluorosulfonic acid PFSA PEMs. Unlike low temperature PFSA MEAs, high temperature PA-doped PBI membranes do not need to be hydrated, and therefore, do not require an external humidification of the gases. Additionally, running at high temperatures generally improves electrode kinetics and proton conductivities while requiring smaller heat exchangers. For PBI fuel cell science to transition into commercially available products, the reliability of PBI fuel cell stacks needs to meet specific requirements. The Department of Energy (DOE) specified durability targets of >5,000 h (>150,000 miles) of automotive fuel cell operation and >40,000 h for stationary applications for 2010. Primarily, the durability of the fuel cell stack dictates the durability of the entire system [91]. In depth durability studies of PBI MEAs have been performed [56, 61, 68, 87, 92–94] to evaluate the viability of commercial PBI fuel cells. In addition to fuel impurity and PA retention tests, load, thermal, and shutdown-startup cycling tests are commonly performed to evaluate the MEAs.

p-PBI MEAs have displayed a relatively high resistance to carbon monoxide and sulfur contaminants [87, 92, 95, 96]. While Nafion and other traditional low-temperature PEM fuel cells are often poisoned by small amounts of carbon monoxide (5–50 ppm) in the fuel or oxidant, *p*-PBI and other PBI membranes have been shown to perform with minimal voltage loss in 10^4 ppm of carbon monoxide. Operating the fuel cell at 180 °C with a load of 0.2 A cm^{-2} with a reformate gas (70% H_2, 1.0% CO, and 29% CO_2), the voltage loss was only 24 mV as compared to pure hydrogen [29]. This decrease in voltage occurred as a result of fuel dilution and carbon monoxide poisoning. As explained in section "Introduction to Polybenzimidazole Fuel Cell Sustainability," the cell is able to resist poisoning because the high operating temperatures allow for reversible binding of carbon monoxide from the catalyst. Details on the CO adsorption isotherms in the presence of hydrogen under fuel cell operation conditions between 150 °C and 190 °C can be found in literature [96]. Similarly, Garseny et al. [95] reported that a PBI MEA from BASF Fuel Cell GmbH (Celtec-P Series 1000) is 70 times more resistant to sulfur contaminants than Nafion MEAs. Using air contaminated with 1 ppm H_2S or SO_2 as the oxidant, the performance of Nafion decreased by 82.9% while the performance of the Celtec-P MEA decreased by <2%. Garseny et al. proposed that H_2S is converted to SO_2, and that SO_2 adsorbs onto the Pt catalyst surface. At temperatures above 140 °C, this SO_2 is desorbed and flushed out of the system. Schmidt and Baurmeister showed that the H_2S tolerance of PBI-based Celtec P1000 MEAs is in the range of 10 ppm [92], a value significant larger than typical fuel processing catalyst can tolerate. More than 3000 h operation in reformate with 5 ppm H_2S and 2% CO was demonstrated. Overall, *p*-PBI-based fuel cells can resist contaminant poisoning far better than traditional low-temperature PEM fuel cells, an effect which can mainly be ascribed to the operation temperature between 150 °C and 190 °C.

Under continuous operation and appropriate stack design and components, the PBI membranes retain phosphoric acid extremely well. Long-term performance tests show that *p*-PBI fuel cells can operate for over two years with minimal performance degradation (Fig. 17). This durability is attributed to the unique nature of PBI membrane formed by the PPA process, which allows it to retain PA under continuous operating conditions. The amount of PA lost from the *p*-PBI MEA per h was approximately 10 ng h^{-1} cm^{-2}, which is equivalent to a 50 cm^2 cell losing 8.74 mg PA after two years of operation. Such a small loss strongly suggests that the life span of a *p*-PBI PEM fuel cell would not be significantly influenced by PA depletion.

Phosphoric acid loss was also monitored during a selection of dynamic durability tests,

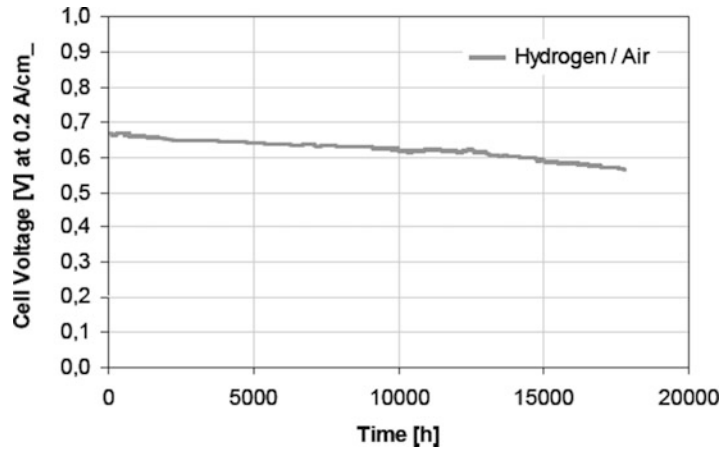

Polybenzimidazole Fuel Cell Technology: Theory, Performance, and Applications,
Fig. 17 Long-term durability test of *p*-PBI MEA at 160 °C using hydrogen/air without humidification

including load and thermal cycling tests [87]. A single load cycle test involved measuring the voltage at 160 °C under at three different loads: open circuit voltage (OCV), 0.2 A cm^{-2}, and 0.6 A cm^{-2}. Air and pure hydrogen were supplied to the MEA as oxidant and fuel, respectively. The voltage of the MEA was measured at OCV for 2 min, followed by 0.2 A cm^{-2} for 30 min and then 0.6 A cm^{-2} for 30 min. A total of 500 load cycles were performed on a *p*-PBI MEA, and the results indicated that larger loads corresponded to an increased PA loss rate (approximately 20 ng h^{-1} cm^{-2}). Thermal cycling tests were performed by measuring the voltage of the MEA with a constant applied current density of 0.2 A cm^{-2} while either cycling the temperature between 120 °C and 180 °C (for a high temperature cycle) or between 80 °C and 120 °C (for a low temperature cycle). Both the high and low temperature cycles were performed 100 times each. The results showed that higher temperatures were associated with an increased PA loss rate (almost 70 ng h^{-1} cm^{-2} for the high temperature cycle and 20 ng h^{-1} cm^{-2} for the low temperature cycle). It was proposed that at the higher load and temperature conditions, more water is generated at the cathode. By means of a steam distillation mechanism, an increased amount of PA is lost from the MEA. As indicated by both cycling tests, phosphoric acid loss becomes a significant factor of cell degradation only under extreme conditions.

Shutdown-startup cycling tests have been extensively studied by Schmidt and Baurmeister of BASF Fuel Cell GmbH [61, 68]. Two PBI-based PEFC Celtec-P 1000 MEAs were tested under different operation modes; one was run under shutdown-startup cycling parameters (12 h shutdown followed by operation for 12 h at 160 °C under a load of 0.2 A cm^{-2}) while the other was continuously operated at 160 °C under a load of 0.2 A cm^{-2}. Both MEAs were operated for more than 6000 h, during which the shutdown-startup cycling MEA underwent more than 270 cycles. While the continuously operating MEA had an average voltage degradation rate of roughly 5 μV h^{-1}, the cycling MEA averaged a voltage degradation of 11 μV h^{-1} or 0.2 mV $cycle^{-1}$. This increase in voltage degradation was attributed to an increased corrosion of the cathode catalyst support, thereby significantly increasing the cathodic mass transport overpotential. The observed corrosion was a result of a reverse-current mechanism that occurs under shutdown-startup cycling conditions [97].

Illustrated by the previously discussed durability tests, *p*-PBI MEAs have been shown to be physically and chemically robust. Highly resistant to fuel contaminants, PBI MEAs are resistant to poisoning effects that would typically expunge a low temperature PFSA fuel cell system. Long term steady-state and dynamic durability tests showed that PA loss typically is not a cause of cell degradation. Additionally, Schmidt and Baurmeister showed that PBI MEAs are susceptible to cell degradation under extreme shutdown-startup conditions. Overall, *p*-PBI MEAs have

exhibited much potential for use in fuel cell systems.

Advances in PBI MEA Manufacturing

As previously discussed, the manufacturing processes of PBI-based fuel cells need to be improved to make fuel cells a viable commercial product. To put this requirement into perspective, the United States Department of Energy has set a goal of producing 500,000 fuel cell cars each year. If these vehicles are powered using current *p*-PBI membranes, this goal requires the production of seven MEAs per second and approximately 250,000 m^2 of electrode per day. Additionally, the performance of each of these MEAs would need to be tested; this is a process called "burn-in testing." A typical test stand is 25 ft^2, costs roughly $50,000, and can only test one stack of MEAs at a time. If each stack requires a 24 h burn-in test, the test facility size would exceed 34,000 ft^2 and house equipment costing over $68.5 million. Existing manufacturing processes need to be improved in order to reach this goal.

The Center for Automation Technologies and Systems (CATS) at Rensselaer Polytechnic Institute has developed a flexible manufacturing process for BASF Fuel Cell GmbH to accommodate the evolving science of fuel cells [98–100]. If one changes the fuel cell type, size, materials, MEA architecture, design, or application, the manufacturing line could be significantly affected. Therefore, a modular manufacturing line was developed by CATS in 2002 that could produce a large range of MEA sizes (1–1000 cm^2), could handle a wide variety of materials (membranes, gaskets, electrodes, etc.), could assemble these materials in different architectures, and could be expanded to integrate additional systems. Each module could be singularly operated or could operate as a subset of the entire process; this modular construction is shown in Fig. 15. Over the past eight years, this manufacturing line has evolved over three generations of MEA devices (Fig. 18).

Members of CATS continue to make great strides in order to reduce costs and improve the overall efficiency of MEA fabrication. Laser cutting and joining of the PBI membranes both uses less power and delivers tighter tolerances than that of conventional cutting and joining. Ultrasonic technology has also been explored to replace the thermal joining of the three components of an MEA. Preliminary results exhibited a significant reduction in pressing time by approximately 90% in addition to using less energy. Additionally, an automated visual inspection of the MEA has been developed using a high precision motion system, multiple cameras and lighting equipment, and software MAT-LAB 7.0 with Image Processing Toolbox [99]. As fuel cell science continues to evolve, so will the manufacturing processes.

Combined Heat and Power

Stationary combined heat and power (CHP) devices are often considered the primary application of high temperature PBI-based fuel cells. These devices are used to provide both electricity and heat (in the form of hot air or water) to small scale residential homes or large scale industrial plants using hydrogen derived from the widely distributed natural gas network. PBI MEAs are ideally situated for combined heat and power devices because they efficiently provide electricity while generating heat as a byproduct. Furthermore, these devices could be used to provide reliable backup power to residential homes, hospitals, servers, etc.

J.-Fr. Hake et al. [101] compared the conventional generation of heat and electricity to that of small scale combined heat and power generation by high temperature fuel cells, and the results of which are shown in Fig. 19. The small scale CHP devices studied were used to provide electricity, space heat, and warm water to both residential and commercial buildings. The conventional generation of electricity is much less efficient than that of small scale CHP devices due to the issues of transportation and storage. In addition to efficiently converting chemical energy into electrical energy, CHP fuel cell systems further act as a sustainable energy conversion device by reducing the total amount of greenhouse gas emissions. Hake et al. considered the penetration of small scale CHP fuel cell technology into the US

Polybenzimidazole Fuel Cell Technology: Theory, Performance, and Applications, Fig. 18 A portion of the 2002 pilot line depicting its modular construction [98]

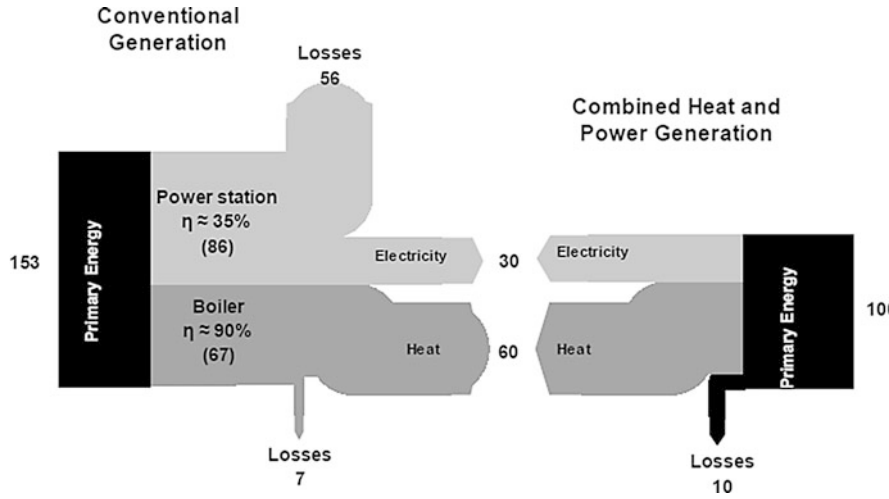

Polybenzimidazole Fuel Cell Technology: Theory, Performance, and Applications, Fig. 19 Side-by-side comparison of conventional generation of heat and electricity to fuel cell combined heat and electricity generation [101]

residential sector market starting in 2014 until a saturation point as a logarithmic function. To improve the accuracy of the study, Hake considered the trends of the Japanese small scale CHP market [101, 102]. A typical CHP device in Japan costs roughly $30,000, but analysts expect the price to drop to $5000 within five years. Analysts also claim that by the year 2050, one in four homes in Japan will run on fuel cells. Also considering current CO_2 emissions, Hake et al. concluded that adoption of this technology in the US could reduce CO_2 emissions by up to approximately 50 million tons by 2050; this corresponds to a 4% reduction in the residential sector.

As the largest producer of PBI MEAs, BASF Fuel Cell (previously PEMEAS) produces *p*-PBI PEM MEAs for a wide variety of fuel cell applications. The Celtec®-P 1000 PEM MEA is typically integrated into either back-up or auxiliary power units and can produce from 0.25 to 10 kW. The MEA is also advertised as maintaining performance for over 20,000 h with only a 6 μV h^{-1}

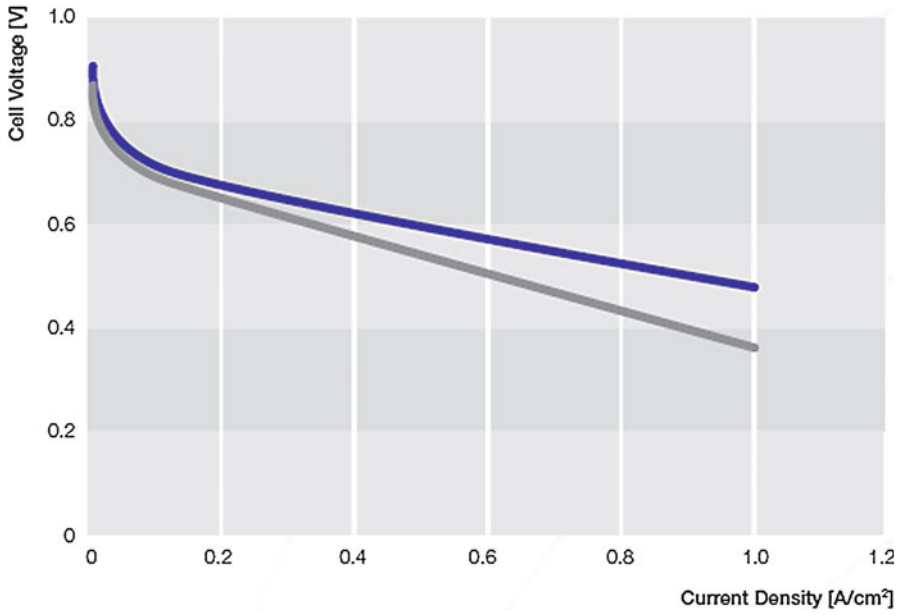

Polybenzimidazole Fuel Cell Technology: Theory, Performance, and Applications, Fig. 20 Polarization curves of a Celtec®-P MEA [103]. The *blue line* represents using hydrogen/air as fuel/oxidant. The *gray line* represents a steam reformate of 70% H_2, 29% CO_2, and 1% CO/Air

voltage drop at 160 °C [98]. The Celtec®-P 2100 PEM MEA is used in stationary CHP systems and is capable of producing 0.74–10 kW. The MEA has a long term stability of over 20,000 h under both steady state and cycling conditions (300 shutdown-startup cycles with 13 μ h^{-1} voltage drop). Polarization curves of a Celtec®-P MEA at 160 °C using an active area of 45 cm^2 are shown in Fig. 20. PBI-based CHP devices have been commercially test marketed by a variety of companies, including Serenergy, Plug Power, and ClearEdge Power, although large scale adoption has not yet been achieved.

Furthermore, Celtec®-P 1100W is an improved version to Celtec®-P 1000. It provides more uniformity and a greater degree of manufacturing readiness (Fig. 21) [104].

Plug Power of Latham, New York produced a line of PBI-based small scale CHP devices including the GenSys Blue (Fig. 22) [105]. The GenSys Blue was capable of producing 0.5–5 kW of continuous output and capable of reducing home energy costs by 20–40%. An autothermal (ATR) reformer reacts to natural gas (methane) with oxygen and carbon dioxide to produce hydrogen gas that fuels the PEM stack. An inverter was used to improve the efficiency of the CHP device by specifically supplying enough energy to power the home, thereby minimizing energy losses and reducing CO_2 emissions by 25–35%. Additionally, an integrated peak heater ensures proper heating of the entire home. More recently, Plug Power has focused on integrating low temperature PEMFC's into forklift trucks.

Serenergy, which is based in Hobro, Denmark, also produced a PBI-based fuel cell CHP devices [106]. Serenergy's Serenus 166 Air C v2.5 and 390 Air C v2.5 micro-CHP modules nominally produce 1 and 3.5 kW, respectively. While the 166 model was comprised of one MEA stack of 65 cells, the 390 model uses three MEA stacks each with 89 cells. Both of these systems were able to tolerate fuel impurities up to 5% CO concentrations and 10 ppm H_2S at 160 °C. Because the excess energy can be used to heat up air or water, Serenergy claims that over 80% of the total heat and power generated can be used and that the system efficiency is as high as 57% (the efficiency data was not available). These systems can also be used as auxiliary energy conversion devices.

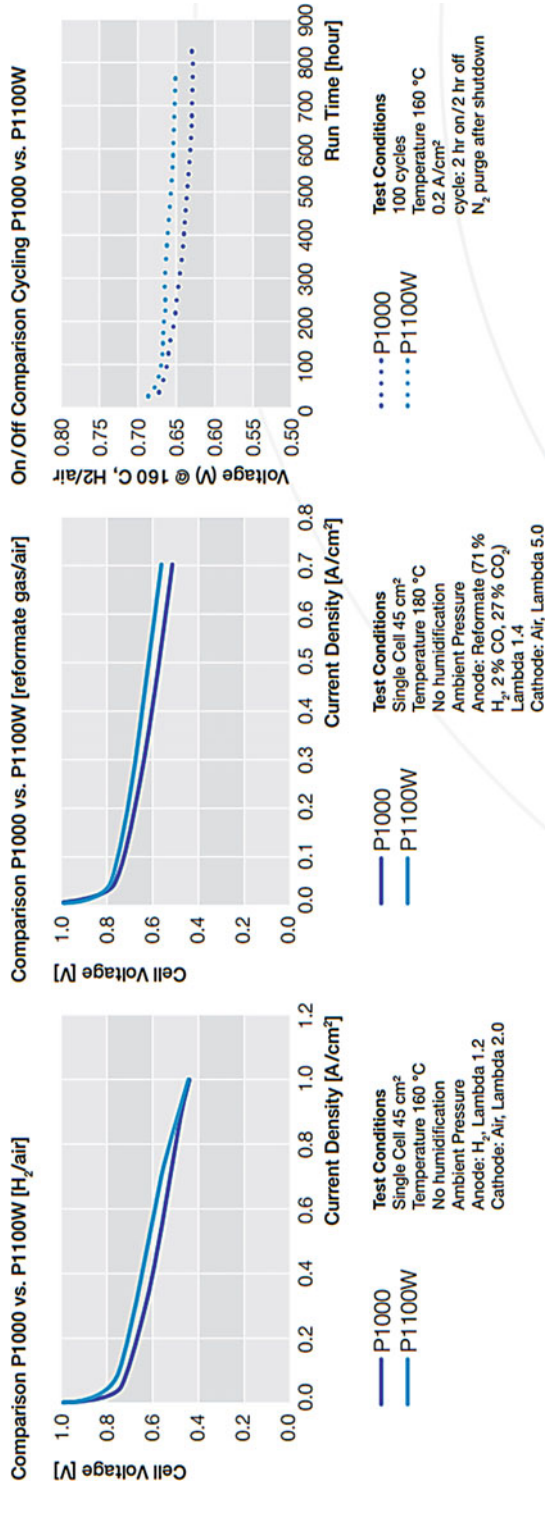

Polybenzimidazole Fuel Cell Technology: Theory, Performance, and Applications, Fig. 21 Comparison of Celtec®-P 1100W and Celtec®-P 1000 [104]

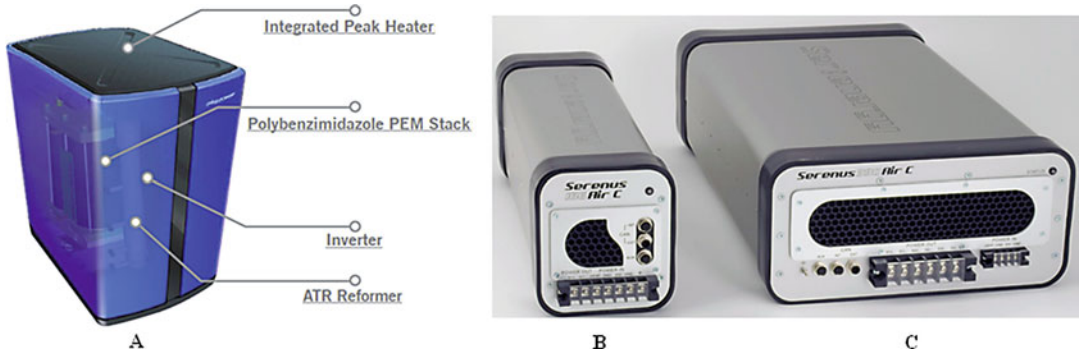

Polybenzimidazole Fuel Cell Technology: Theory, Performance, and Applications, Fig. 22 Plug Power's GenSys *Blue* (**a**), Serenergy's Serenus 166 Air C v2.5 (**b**), and Serenergy's Serenus 390 Air C v2.5 (**c**) CHP fuel cell devices [105, 106]

ClearEdge Power produced a line of small scale CHP devices, one of which is the ClearEdge5 [107]. Capable of producing 5 kW h^{-1} and up to 20,000 BTU h^{-1} while running at 150 °C, the ClearEdge5 couples a methane reformer to a PBI fuel cell stack using MEAs provided by BASF Fuel Cell GmbH. ClearEdge advertised that the CHP device could reduce utility bills by up to 50% and cut CO_2 emissions by over 33%. Annually, the device was capable of producing 43,000 kWh in electricity and 50,000 kWh (equivalent) in heat. Similar to other CHP devices, the ClearEdge5 offered at-home production of energy, thereby eliminating the losses associated with transferring the energy. However, ClearEdge Power closed operations in 2014.

In 2016 the fuel-cell industry had an estimated total worth of $3.6 billion and is expected to grow into a $25.5 billion market by 2024, according to research from Global Markets Insight [108]. With that said, many of the major players listed above are no longer in existence or have very little impact on the industry. For example, BASF-Fuel Cell has reduced its market share considerably and now only supplies Celtec®-P 1100W, leaving only Plug Power Inc. and FuelCell Energy Inc. as the major market contributers. However, despite the bullish predictions neither of these two have turned a significant profit. Currently there is uncertainty for the fuel cell technology market, as part of the alternative-energy sector. Hydrogen and fuel companies do not boast the same government incentives as solar and wind firms, however, if this is levied in the future there might be a possible surge in growth of the technology. With emerging needs of sustainable, clean energy in other countries, like China who has invested $100 billion into fuel-cell energy to date, there are other possible avenues for the technology to grow. Fuel cells still remain a viable option for clean energy and to reduce dependence on fossil fuels, leaving hope that they might be an integral part of the growing alternative energy sector [108]. With that said, the research and development on fuel cell technologies has laid the foundation for other possible devices that could alleviate the use of fossil fuels. These include both hydrogen pumping, which can be used to purify hydrogen from a mixed gas stream, as well as the hybrid sulfur cycle, which is an enticing thermal-electrochemical process used for the production of pure hydrogen. These will be discussed more in depth in sections "H_2 Pump" and "The HyS Cycle."

Automotive Transportation

Producing 1.9253 billion metric tons of carbon dioxide, which is roughly 33% of the United States' total carbon dioxide emissions, the transportation sector was the largest contributor to pollution in 2008 [109]. According to another 2009 study by the U.S. Department of Energy [3], all transportation in the US produced

approximately 1850 million metric tons of carbon dioxide emissions. Considering both of these facts, one can conclude that a more sustainable energy source could significantly reduce the carbon footprint of the transportation sector. For the transition of fuel cell science into a viable commercial product to occur, the U.S. Department of Energy has set numerous targets for automotive fuel cell systems. Because a typical internal combustion engine costs roughly $25–35/kW, a fuel cell system will need to cost roughly $30/kW to become competitive enough to penetrate the US market. Furthermore, the system must be durable enough to operate for at least 5000 h (or roughly 150,000 miles). Additional issues of system size and management of air, heat, and water will also play a role in automotive fuel cell viability.

Over the past decade, fuel cell technology has been adapted by the major automotive industries as a cleaner, more efficient method of providing energy to vehicles. In addition to the issue of fuel cell automotive viability, issues of hydrogen sources, hydrogen storage, and fueling stations continue to be addressed and solved. The California Fuel Cell Partnership (CaFCP) is a collaboration of auto manufacturers, energy providers, government agencies, and fuel cell technology companies to promote the commercialization of fuel cell vehicles. In 2009, California had only six public hydrogen fueling stations that were used to fuel roughly 200 vehicles [90]. To date, there are 28 fueling stations open for retail business throughout California and 17 more are under construction. The State of California committed funding to design, build, and provide operation and maintenance support for 100 hydrogen stations [110]. The hydrogen used to fuel these stations can be domestically produced as either a low carbon fuel or potentially as a zero-carbon fuel when produced from renewable sources (such as splitting water into oxygen and hydrogen with solar energy). According to California regulations, at least 33% of the hydrogen must come from such renewable sources [111].

SunHydro, one of the world's first hydrogen fueling station chains, has set a goal of providing fueling stations along the entire east coast of the US. Using solar cell technology, every SunHydro station will harvest solar energy to electrolytically split water into hydrogen and oxygen gases. This process is extremely sustainable and will create much less greenhouse gas emissions. This hydrogen highway will stretch from Scarborough, ME to Miami, FL and consist of eleven stations. Each station will cost an estimated $2–3 million to construct and will be paid for by private funders. Currently there is one hydrogen refueling station open for retail use in Wallingford, Connecticut with plans for a second station to be opened in Braintree, Massachusetts [112].

Over the past decade, many automotive and fuel cell industries have used PBI technology in the development of fuel cell vehicles. In November of 2008, Volkswagen unveiled the VW Passat Lingyu at a Los Angeles Auto Show [113]. The VW Lingyu uses an AB-PBI based fuel cell stack that utilizes a trade-secret coating that helps prevent PA from leeching out of the membrane. Metha Energy Solutions, in cooperation with Serenergy, revealed a hybrid electric/fuel cell vehicle in December of 2009 [114]. In this system, a methanol reformer is used to provide hydrogen to the PBI-based fuel cell. It was advertized that this vehicle could travel up to 310 miles on one tank of gas and takes only 2 min to refuel. EnerFuel, a subsidiary of Ener1, has also recently produced a hybrid electric/fuel cell vehicle. The EnerFuel EV uses a reformed methanol PBI fuel cell that works in conjunction with a lithium ion battery. The lithium battery is used to start the vehicle and to power the vehicle while driving, while the fuel cell system produces 3–5 kW to continuously recharge the battery. These fuel cell systems would not generate enough power to drive the vehicle but would act as a range extender for the battery system. The target market of the EnerFuel EVs is not for those who drive 200+ miles daily but instead for those with short daily commutes.

In July of 2009, the German Aerospace Center demonstrated that fuel cells have the potential of powering air-transportation vehicles [115, 116]. Designed in cooperation with Lange Aviation, BASF Fuel Cell, DLR Institute for Technical

Thermodynamics, and Serenergy, the Antares DLR-H_2 became the world's first piloted aircraft with a propulsion system powered only by PBI-based fuel cells. Besides creating zero CO_2 emissions during flight, the aircraft also generates much less noise than other comparable motor gliders. Using a fuel cell stack capable of producing up to 25 kW, the Antares DLR-H_2 has a cruising range of 750 km (or 5 h) and can travel at speeds up to 170 km h^{-1}. Similar fuel cell systems could be coupled with current commercial and military aircrafts as auxiliary power units (APUs) to improve fuel efficiency.

Portable

Microelectricalmechanical (MEM) systems utilizing methanol reformers and PBI fuel cells have been developed for portable use. These devices are generally used to generate power in the range of 5–50 W for laptops, communication systems, and global positioning systems. Compared to batteries that offer equivalent amounts of power, these micro-fuel cell systems are lighter, generate less waste, and are overall more cost effective. Similar to other reformed methanol/PBI fuel cell systems, these MEMS are a sustainable technology by reducing the amount of greenhouse gases produced per unit of electricity generated.

UltraCell of Livermore, CA is a well-known producer of PBI MEM fuel cell systems. Funded and field tested by the U.S. Army, the UltraCell XX25 is capable of providing 25 W of continuous maximum power [117]. Depending on the size of the fuel cartridge, the device is capable of delivering 20 W of continuous power from 9 h to 25 days. The fuel cartridge weighs less than a pound and the XX25 MEM system has been shown to power radio gear, mobile computer systems, communication devices, and a variety of other electrical devices. The XX25 provides roughly 70% in weight savings when compared to a typical battery on a 72-h mission (1.24 kg without the cartridge) and is rugged enough to operate in extremely cold or hot environments. In addition, it meets OSHA standards for safe indoor and in-vehicle use. Similar to the XX25, the newly developed UltraCell XX55 is capable of generating 55 W of continuous power for up to two weeks using the largest fuel cartridge [118]. Only 0.36 kg heavier than the XX25, the XX55 has an optional battery module that can provide a peak power output of 85 W. Similar to the XX25, it is a very rugged device that can be used essentially in any conditions [118].

Larger than the Ultracell devices, Serenergy test marketed the Serenus E-350, which was a reformed methanol/fuel cell hybrid with an approximate mass of 11 kg. At nominal power levels, it was capable of producing approximately 350 W [119]. The device was fueled by a 60–40 methanol-deionized water mixture. It took approximately 45 min to start-up, at which point it consumed fuel at a rate of 0.45 L h^{-1}. Serenergy has, since then, stopped producing the smaller device and replaced it with a midsized model; the H_3 2500 and 5000 (both weighing around 65–75 kg) [120].

H_2 Pump

Efficient purification of hydrogen is becoming a common interest in both the industrial and energy sectors. In particular, technology which can efficiently purify, pump, and pressurize hydrogen at low to moderate flow rates is needed but is not readily available. Of course, there are existing methods for hydrogen purification which include various combinations of mechanical compression with cryogenic cleanup, palladium membranes, pressure swing absorption, and passive membrane separators to name a few. However, these technologies are challenged by certain limitations: (1) cryogenic cleanup produces high purity hydrogen, but requires costly refrigeration equipment and is suitable for very large-scale specialty applications; (2) palladium membrane purification can be fairly simple in design and construction but requires pressurization to drive the hydrogen separation process and suffers from poor utilization when purifying hydrogen from gases containing low fractions of hydrogen; (3) pressure swing absorption

(PSA) is widely used in high volume industrial processes and relies on large, mechanical components that are subject to frequent maintenance and inherent inefficiency. Such devices are not easily scaled to smaller sizes or localized generation/purification needs. Furthermore, it is important to state that all of the above processes require expensive, high maintenance, compressors.

Electrochemical pumping is not a new concept and has in fact been utilized as a diagnostic technique within the electrochemical industry for years. General Electric developed this concept in the early 1970s [121].

The use of polymer electrolyte membranes for electrochemical hydrogen compression has been demonstrated in water electrolysis (H_2 generation) devices at United Technologies Corporation, reaching 3000 psi_a [122], as well as studied in academic institutions [123]. The electrochemical hydrogen pump, first developed in the 1960s and 1970s, was derived from the original proton exchange membrane fuel cell efforts. The concept is simple, requires little power, and has been shown to pump hydrogen to high pressures. In the original work, the membrane transport medium was a perfluorosulfonic acid (PFSA) material, similar to the material used in many fuel cells today. The process is quite elegant in that like a fuel cell, molecular hydrogen enters the anode compartment, is oxidized to protons and electrons at the catalyst, and then the protons are driven through the membrane while the electrons are driven through the electrically conductive elements of the cell (Fig. 23).

The major difference in this cell as compared to a fuel cell is that the pump is operated in an electrolytic mode, not galvanic, meaning that power is required to "drive" the proton movement. Once the protons emerge from the membrane at the cathode, they recombine to form molecular hydrogen. Thus, hydrogen can be pumped and purified in a single step with a non-mechanical device. The pump concept builds upon the understanding of proton transport membranes. The overall chemicals are described by Eq. 1:

$$\begin{aligned} &\text{Anode} : H_2 \rightarrow 2H^+ + 2e^+ \\ &\text{Cathode} : 2H^+ + 2e^- \rightarrow H_2 \\ &\text{Total Reaction} : H_2(\text{anode}) \rightarrow H_2(\text{cathode}) \end{aligned} \tag{1}$$

The cell voltage between the anode and cathode can then be described by the Eq. 2. The Nernst potential, E_{Nernst}, is given by the Nernst Eq. 3, where E° is the standard potential of a hydrogen reaction, R is the gas constant, T is the temperature in Kelvin, F is Faraday's constant, and p_{cathode} and p_{andode} are the partial pressures of hydrogen at the anode and cathode respectively.

$$E = E_{\text{Nernst}} - E_{\text{polarization}} - E_{\text{ohmic}} \tag{2}$$

$$E_{\text{Nernst}} = E^{\circ} - \frac{RT}{2F} \ln \frac{p_{\text{cathode}}}{p_{\text{anode}}} \tag{3}$$

$E_{\text{polarization}}$ is the polarization overpotential which is the sum of the polarization overpotentials at the anode and cathode. This can be described using the Butler-Volmer equation. The polarization overpotential can be approximated at low overpotentials, Eq. 4, where R is the gas constant, T is the temperature in Kelvin, F is Faraday's constant, i is the current density, and i_0 is the exchange current density.

$$E_{\text{polarization}} = \frac{RTi}{2Fi_0} \tag{4}$$

Clearly, the proton conducting membrane properties are critical. Desirable properties include: high proton conductivity, mechanical stability, low solubility and permeability of impurity gases, and sufficient operating temperature to support tolerance to impurities (CO and H_2S) found in reformed gases. The application of the PBI membrane to electrochemical hydrogen pumping provides high proton conductivity (0.2–0.4 S/cm), mechanical stability, enhanced gas separation, and up to 180 °C operation. The high operating temperature eliminates water management difficulties typically experienced with the low operating temperatures of PSFA membranes while also providing tolerance to poisonous gas species such as

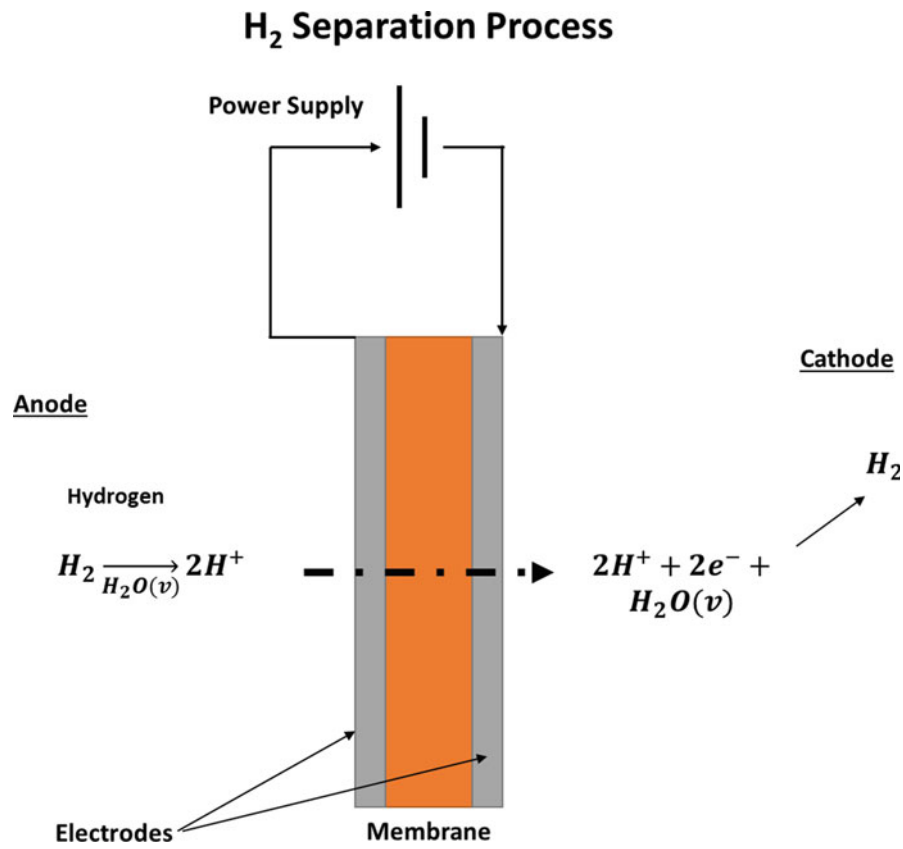

Polybenzimidazole Fuel Cell Technology: Theory, Performance, and Applications, Fig. 23 Polymer electrolyte based hydrogen electrolysis

CO. This is a crucial quality in electrochemical hydrogen pumping as many of the common impurities being removed from the feed stream are known to poison the catalyst. As such, the PBI membrane and electrode assembly represents a significant new opportunity and paradigm shift in electrochemical hydrogen pumps as well as in advancing the science of hydrogen separation, purification, and pressurization. This concept has been evaluated and demonstrated in recent work using PBI membranes [124]. The hydrogen pump was shown to operate with fairly low power requirements and generally needed less than 100 mv when operating at 0.2–0.4 A/cm^2. This was accomplished without the critical water management commonly encountered in low temperature, water-based membranes. The cathodic flow of hydrogen from the device was nearly identical to the theoretical Faradic flows. This suggests that the hydrogen pump could have applications as a hydrogen metering device since the hydrogen flow could be easily and accurately controlled by the current of the power source. The initial work reported devices that could operate for several thousand hours with little change in the operating parameters. This would be expected from the related work on PBI membranes for fuel cells which show outstanding long-term durability. In fuel cell applications, the ability to operate at high temperatures provides benefits for gas cleanup and durability on reformed fuels. In hydrogen pump applications, this tolerance to fuel impurities enables the hydrogen pump to purify hydrogen from hydrogen gas feeds containing such impurities. Figure 24 shows the operation of a PBI-based hydrogen pump operating on pure hydrogen, as well as two different synthetic reformates. The flow rates are nearly unaffected by the

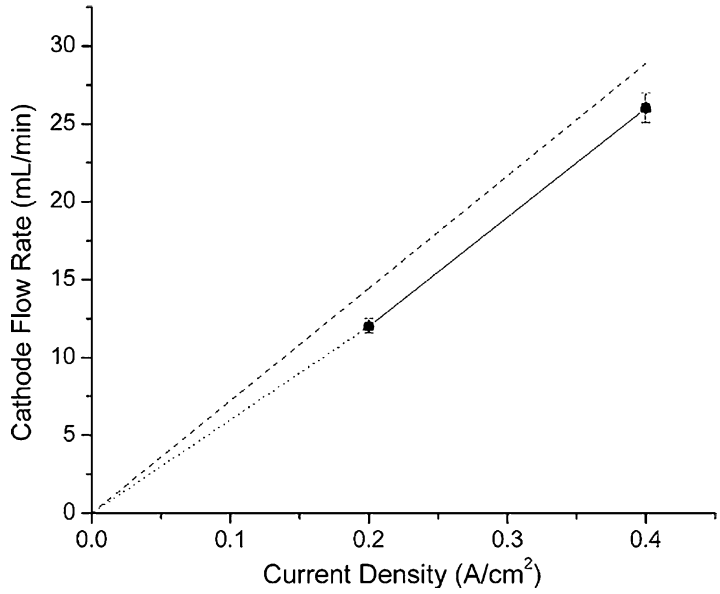

Polybenzimidazole Fuel Cell Technology: Theory, Performance, and Applications, Fig. 24 The cathodic flow rates of a hydrogen pump operated at 160 °C and 0% relative humidity and fueled by pure hydrogen (*unfilled squares*), a reformate gas comprised of 35.8% H_2, 11.9% CO_2, 1906 ppm CO, and 52.11% N_2 (*filled circles*), and a reformate gas comprised of 69.17% H_2, 29.8% CO_2, and 1.03% CO (*filled triangles*). The values are nearly identical, and thus, the symbols appear superimposed. The dotted line represents the theoretical flow rate at 100% efficiency [124]

composition of the gas feed at the various operating conditions (the data points are superimposed for the different gases). The data demonstrates that the pump was capable of operating at high CO levels (1% in this work) and extracting hydrogen from dilute feed streams (<40% hydrogen). Additionally, the hydrogen pump was capable to producing hydrogen with purities greater than 99%, with the final purity dependent on operating conditions. This device could play a prominent role for both the current industrial hydrogen users, as well as in a future economy that is more heavily reliant on hydrogen as an energy carrier. Commercial development of this device is underway.

The HyS Cycle

More recently, the hybrid sulfur thermochemical cycle has drawn a great amount of attention due to its potential to provide clean hydrogen on a large scale using considerably less energy than water electrolysis. The hybrid sulfur (HyS) process contains two steps: (1) a high temperature decomposition of sulfuric acid to produce sulfur dioxide, oxygen, and water and (2) a low temperature electrochemical oxidation of sulfur dioxide in the presence of water to form sulfuric acid and gaseous hydrogen. The entire process recycles sulfur compounds which leave a net reaction splitting water into hydrogen and oxygen. Herein we describe advancements in the low temperature sulfur oxidation step that could be coupled with next generation solar power plants or high temperature nuclear reactors.

Since the HyS process involves the transfer of protons it is not surprising that proton exchange membranes (PEMs) are the most investigated materials. Historically, Nafion has been usually the most widely studied due to its availability. Nation's performance in the HyS electrolyzer has been thoroughly examined with the prediction of mass transport through the membrane as a function of operating potential and other design variables. Nafion does, however, have many drawbacks including the inability to operate at elevated temperatures (above 100 °C) and since water is needed for its conductivity, there is

decreased performance at high acid concentrations or low water concentrations [125].

Polybenzimidazole (PBI) membranes are high temperature PEMs that are imbibed with acid as its electrolyte. We have shown that PBI membranes are a good alternative to Nafion in fuel cells and offer a solution to the HyS process as an avenue to higher temperature operation, which minimizes voltage losses, as well as the ability to perform under high acid concentration conditions that allow for reduced energy demands necessary for water separation. Weidner et al. show the successful operation of the HyS electrolyzer using sulfuric acid doped PBI membranes and have determined that the area-specific resistance of sulfonated PBI (s-PBI) compares favorably with Nafion, yet is not adversely affected by concentrated sulfuric acid conditions within the electrolyzer. Importantly, the PBI-based cell could be operated at low pressures and without significant water dilution of the sulfuric acid produced. Additionally, a model for high temperature and high-pressure operation of the s-PBI membrane in the electrolyzer has been constructed allowing for further analysis of the system to determine operating conditions for economically viable operation [125, 126].

Conclusions and Future Directions

After approximately 15 years of development, PBI chemistries and the concomitant manufacturing processes have evolved to produce commercially available MEAs. PBI MEAs can operate reliably without complex water humidification hardware and are able to run at elevated temperatures of 120–180 °C due to the physical and chemical robustness of PBI membranes. These higher temperatures improve the electrode kinetics and conductivity of the MEAs, simplify the water and thermal management of the systems, and significantly increase their tolerance to fuel impurities. Membranes cast by a newly developed PPA Process possessed excellent mechanical properties, higher PA/PBI ratios, and enhanced proton conductivities as compared to previous methods of membrane preparation.

The robustness of *p*-PBI membranes cast by the PPA Process has been tested and characterized by a variety of methods. Under a constant load, *p*-PBI has been shown to perform for well over two years with very little reduction in performance. Using synthetic reformates, *p*-PBI MEAs have demonstrated excellent resistances to impurities such as CO, CO_2, and SO_2. *p*-PBI membranes have also been shown to retain PA extremely well, and evidence strongly suggests that this small rate of PA loss would not significantly influence the life span of a MEA. Load, thermal, and shutdown-startup cycling tests of *p*-PBI fuel cells have also indicated comparable or improved results over other commercially available fuel cell systems. *p*-PBI is the most common polymer in PBI-based fuel cell systems, although AB-PBI, *m*-PBI, and other derivatives have been investigated. Recently developed 2OH-PBI, which to date has the highest recorded proton conductivity of all other PBIs, offers much potential for future fuel cell use.

Many fuel cell manufacturers are now considering the benefits of high temperature PBI fuel cells. BASF Fuel Cell, the largest producer of PBI MEAs, has been in operation since March of 2007. BASF offers a wide variety of MEAs for stationary systems (combined heat and power, backup generators, etc.) and portable systems (transportation, microelectricalmechanical systems, etc.). Other companies, such as Plug Power, Serenergy, ClearEdge Power, and UltraCell have incorporated commercially available MEAs into commercial fuel cell systems. Additionally, Danish Power Systems has expanded its offerings and its presence in offering BI-based MEAs with improved durability. Companies such as H_2 Pump LLC developed electrochemical pumping devices that use PBI membranes for the purification of hydrogen gas. Using various reformate gases, the devices have been shown capable of operating at high gas contamination levels and low hydrogen concentrations. Depending on operating conditions, the purity of the extracted hydrogen gas can be greater than 99%. In transportation applications, PBI-based fuel cells show great promise as APUs or range extenders for battery powered electric vehicles.

Bibliography

1. EIA (2016) International Energy Outlook 2016. U.S. Energy Information Administration
2. EIA (2009) Annual Energy Review 2008. U.S. Energy Information Administration
3. EIA (2011) Emissions of greenhouse gases in the United States 2009. U.S. Energy Information Administration
4. EPA (2017) Overview of greenhouse gases: carbon dioxide emissions. U.S. Environmental Protection Agency. http://safetynet.dropmark.com/304772/6659915
5. Wainright J, Wang J, Weng D, Savinell R, Litt M (1995) Acid-doped polybenzimidazoles: a new polymer electrolyte. J Electrochem Soc 142(7): L121–L123
6. Dippel T, Kreuer KD, Lassègues JC, Rodriguez D (1993) Proton conductivity in fused phosphoric acid; A 1H/31P PFG-NMR and QNS study. Solid State Ion 61(1):41–46. https://doi.org/10.1016/0167-2738(93)90332-W
7. Bozkurt A, Ise M, Kreuer KD, Meyer WH, Wegner G (1999) Proton-conducting polymer electrolytes based on phosphoric acid. Solid State Ion 125(1):225–233. https://doi.org/10.1016/S0167-2738(99)00179-4
8. Weber J, Kreuer K-D, Maier J, Thomas A (2008) Proton conductivity enhancement by nanostructural control of poly(benzimidazole)-phosphoric acid adducts. Adv Mater 20(13):2595–2598. https://doi.org/10.1002/adma.200703159
9. Melchior JP, Majer G, Kreuer KD (2017) Why do proton conducting polybenzimidazole phosphoric acid membranes perform well in high-temperature PEM fuel cells? Phys Chem Chem Phys 19(1):601–612. https://doi.org/10.1039/c6cp05331a
10. Li Q, Aili D, Hjuler HA, Jensen JO (2016) High temperature polymer electrolyte membrane fuel cells. Springer, NY: 545
11. Mader J, Xiao L, Schmidt T, Benicewicz BC (2008) Polybenzimidazole/acid complexes as high-temperature membranes. Adv Polym Sci 216(Fuel Cells II):63–124
12. Wainright JS, Savinell RF, Litt MH (2003) High temperature membranes. Handbook of fuel cells, vol 3. Wiley, NY, pp 436–446
13. Colomban P (1992) Proton conductors: solids, membranes, and gels – materials and devices. Cambridge University Press, Cambridge
14. Xiao L, Zhang H, Scanlon E, Ramanthan LS, Choe EW, Rogers D, Apple T, Benicewicz BC (2005) High-temperature polybenzimidazole fuel cell membranes via a sol-gel process. Chem Mater 17(21):5328–5333
15. Jayakody JRP, Chung SH, Durantino L, Zhang H, Xiao L, Benicewicz BC, Greenbaum SG (2007) NMR studies of mass transport in high-acid-content fuel cell membranes based on phosphoric acid and polybenzimidazole. J Electrochem Soc 154(2): B242–B246. https://doi.org/10.1149/1.2405726
16. Seel DC, Benicewicz BC, Xiao L, Schmidt TJ (2009) High-temperature polybenzimidazole-based membranes. Handbook of fuel cells, vol 5. Wiley, NY, pp 300–312
17. Litt M, Ameri R, Wang Y, Savinell RF, Wainright JS (1999) Polybenzimidazole/phosphoric acid solid polymer electrolytes: mechanical and electrical properties. Mater Res Soc Symp Proc 548:313–323
18. Zhang H (2004) Novel phosphoric acid doped polybenzimidazole membranes for fuel cells. Ph.D. thesis, Rensselaer Polytechnic Institute, Troy, December
19. Li Q, Hjuler HA, Bjerrum NJ (2001) Phosphoric acid doped polybenzimidazole membranes: physiochemical characterization and fuel cell applications. J Appl Electrochem 31(7):773–779
20. Zhai Y, Zhang H, Liu G, Hu J, Yi B (2006) Performance degradation studies on PBI/H3PO4 high temperature PEMFC and one-dimensional numerical analysis. J Electrochem Acta 52(2):394–401
21. Kongstein OE, Berning T, Borresen B, Seland F, Tunold R (2007) Polymer electrolyte fuel cells based on phosphoric acid dopted polybenzimidazole (PBI) membranes. Energy 32(4):418–422
22. Kim H, Cho SY, An SJ, Eun YC, Kim J, Yoon H, Kweon H, YEW KH (2004) Synthesis of poly (2,5-benzimidazole) for use as a fuel-cell membrane. Macromol Rapid Commun 25(8):894–897
23. Asensio JA, Gomez-Romero P (2005) Recent developments on proton conducting poly (2,5-benzimidazole) (AB-PBI) membranes for high temperature polymer electrolyte membrane fuel cells. Fuel Cells 5(3):336–343
24. Li Q, Jensen JO (2008) Membranes for high temperature PEMFC based on acid-doped polybenzimidazoles. Membr Technol 2:61–96
25. Asensio JA, Borros S, Gomez-Romero P (2004) Polymer electrolyte fuel cells based on phosphoric acid-impregnated poly(2,5-benzimidazole). J Electrochem Soc 151(2):A304–A310
26. Chen R (2004) Unpublished work. Rensselaer Polytechnic Institute, Troy
27. Yu S (2006) Novel polybenzimidazole derivatives for high temperature PEM fuel cells. Ph.D. thesis, Rensselaer Polytechnic Institute, Troy
28. Delano CB, Doyle RR, Miligan RJ (1974) United States Air Force Materials Laboratory. AFML-TR-74-22
29. Yu S, Zhang H, Xiao L, Choe EW, Benicewicz BC (2009) Synthesis of poly (2,2′-(1,4-phenylene) 5,5′-bibenzimidazole) (para-PBI) and phosphoric acid doped membrane for fuel cells. Fuel Cells 9(4):318–324
30. Xiao L (2003) Novel polybenzimidazole derivatives for high temperature polymer electrolyte membrane fuel cell application. Ph.D. thesis, Rensselaer Polytechnic Institute, Troy

31. Xiao L, Zhang H, Jana T, Scanlon E, Chen R, Choe EW, Ramanthan LS, Yu S, Benicewicz BC (2005) Synthesis and characterization of pyridine-based polybenzimidazoles for high temperature polymer electrolyte membrane fuel cell applications. Fuel Cells 5(2):287–295
32. Xiao L, Zhang H, Jana T, Scanlon E, Chen R, Choe EW, Ramanthan LS, Yu S, Benicewicz BC (2004) Synthesis and characterization of pyridine-based polybenzimidazoles for high temperature polymer electrolyte membrane fuel cell applications. Fuel Cells 5(2):287–295
33. Kallitsis JK, Gourdoupi N (2003) Proton conducting membranes based on polymer blends for use in high temperature PEM fuel cells. J New Mat Electrochem Syst 6(4):217–222
34. Faure S, Mercier R, Aldebert P, Pineri M, Sillion B (1996) Gas separation polyimide membranes used to prepare ion-exchange membranes for use in manufacture of fuel cells. France Patent 9,605,707
35. Watari T, Fang J, Tanaka K, Kita H, Okamoto KI, Hirano T (2004) Synthesis, water stability and proton conductivity of novel sulfonated polyimides from 4,4′-bis(4-aminophenoxy)biphenyl-3,3′-disulfonic acid. J Membr Sci 230(1–2):111–120
36. Lufrano F, Gatto I, Staiti P, Antonucci V, Passalacqua E (2001) Sulfonated polysulfone ionomer membranes for fuel cells. Solid State Ionics 145(1–4):47–51
37. Einsla BR, Harrison WL, Tchatchoua C, McGrath JE (2004) Disulfonated polybenzoxazoles for proton exchange membrane fuel cell applications. Polym Prepr 44(2):645–646
38. Gil M, Ji X, Li X, Na H, Hampsey JE, Lu Y (2004) Direct synthesis of sulfonated aromatic poly (ether ether ketone) proton exchange membranes for fuel cell applications. J Membr Sci 234(1–2):75–81
39. Xing P, Robertson GP, Guiver MD, Mikhailenko SD, Kaliaguine S (2004) Sulfonated poly(aryl ether ketone)s containing the hexafluoroisopropylidene diphenyl moiety prepared by direct copolymerization, as proton exchange membranes for fuel cell application. Macromolecules 37(21):7960–7967
40. Gao Y, Robertson GP, Guiver MD, Mikhailenko SD, Kaliaguine S (2004) Synthesis of Copoly(aryl ether ether nitrile)s containing sulfonic acid groups for PEM applications. Macromolecules 37(18):6748–6754
41. Xiao GY, Sun GM, Yan DY, Zhu PF, Tao P (2002) Synthesis of sulfonated poly(phthalazinone ether sulfone)s by direct polymerization. Polym Prepr 43(19):5335–5339
42. Wang F, Hickner M, Kim YS, Zawodzinksi TA, McGrath JE (2002) Direct polymerization of sulfonated poly(arylene ether sulfone) random (statistical) copolymers: candidates for new proton exchange membranes. J Membr Sci 197(1–2):231–242
43. Hickner MA, Ghassemi H, Kim YS, Einsla BR, McGrath JE (2004) Alternative polymer systems for proton exchange membranes (PEMs). Chem Rev 104(10):4587–4611
44. Kim S, Cameron DA, Lee Y, Reynolds JR, Savage CR (1996) Aromatic and rigid rod polyelectrolytes based on sulfonated poly(benzobisthiazoles). J Polym Sci Part A 34(3):481–492
45. Ariza MJ, Jones DJ, Roziere J (2002) Role of post-sulfonation thermal treatment in conducting and thermal properties of sulfuric acid sulfonated poly(benzimidazole) membranes. Desalination 147(1–3):189–194
46. Staiti P, Lufrano F, Arico AS, Passalacqua E, Antonucci V (2001) Sulfonated polybenzimidazole membranes – preparation and physico-chemical characterization. J Membr Sci 188(1):71–78
47. Bae JM, Honma I, Murata M, Yamamoto T, Rikukawa M, Ogata N (2002) Properties of selected sulfonated polymers as proton-conducting electrolytes for polymer electrolyte fuel cells. Solid State Ionics 147(1–2):189–194
48. Asensio JA, Borros S, Gomez-Romero P (2002) Proton-conducting polymers based on benzimidazoles and sulfonated benzimidazoles. J Polym Sci Part A 40(21):3703–3710
49. Sakaguchi Y, Kitamura K, Nakao J, Hamamoto S, Tachimori H, Takase S (2001) Preparation and properties of sulfonated or phosphonated polybenzimidazoles and polybenzoxazoles. J Polym Mater Sci Eng 84:899–900
50. Mader JA, Benicewicz BC (2010) Sulfonated polybenzimidazoles for high temperature PEM fuel cells. Macromolecules 43(16):6706–6715. https://doi.org/10.1021/ma1009098
51. Mader JA, Benicewicz BC (2011) Synthesis and properties of random copolymers of functionalised polybenzimidazoles for high temperature fuel cells. Fuel Cells 11(2):212–221. https://doi.org/10.1002/fuce.201000080
52. He R, Li Q, Xiao GY, Bjerrum NJ (2003) Proton conductivity of phosphoric acid doped polybenzimidazole and its composites with inorganic proton conductors. J Membr Sci 226(1–2):169–184
53. Qian G, Benicewicz BC (2009) Synthesis and characterization of high molecular weight hexafluoroisopropylidene-containing polybenzimidazole for high-temperature polymer electrolyte membrane fuel cells. J Polym Sci, Part A 47(16):4064–4073
54. Yu S, Benicewicz BC (2009) Synthesis and properties of functionalized polybenzimidazoles for high-temperature PEMFCs. Macromolecules 42(22):8640–8648
55. Scanlon E (2005) Polybenzimidazole based segmented block copolymers for high temperature fuel cell applications. Ph.D. thesis, Rensselaer Polytechnic Institute, Troy

56. Schmidt TJ (2006) Durability and degradation in high-temparature polymer electrolyte fuel cells. ECS Trans 1(8):19–31
57. Chen XM, Qian GQ, Molleo MA, Benicewicz BC, Ploehn HJ (2015) High temperature creep behavior of phosphoric acid-polybenzimidazole gel membranes. J Polym Sci Pol Phys 53(21):1527–1538
58. Molleo MA, Chen X, Ploehn HJ, Benicewicz BC (2015) High polymer content 2,5-pyridine-polybenzimidazole copolymer membranes with improved compressive properties. Fuel Cells 15(1):150–159
59. Molleo MA, Chen X, Ploehn HJ, Fishel KJ, Benicewicz BC (2014) High polymer content 3,5-pyridine-polybenzimidazole copolymer membranes with improved compressive properties. Fuel Cells 14(1):16–25
60. Sondergaard T, Cleemann LN, Becker H, Aili D, Steenberg T, Hjuler HA, Seerup L, Li QF, Jensen JO (2017) Long-term durability of HT-PEM fuel cells based on thermally cross-linked polybenzimidazole. J Power Sources 342:570–578
61. Schmidt TJ (2009) High-temperature polymer electrolyte fuel cells: durability insights. In: Buchi FN, Inaba M, Schmidt TJ (eds) Polymer electrolyte fuel cell durability. Springer, New York, pp 199–221
62. Ross PN Jr (1987) Deactivation and poisoning of fuel cell catalysts. In: Petersen EE, Bell AT (eds) Catalyst deactivation. Marcel Dekker, New York
63. Ferreira PJ, la O'GJ, Shao-Horn Y, Morgan D, Makharia R, Kocha S, Gasteiger HA (2005) Instability of Pt/C electrocatalysts in proton exchange membrane fuel cells: a mechanistic investigation. J Electrochem Soc 152(11):A2256–A2271
64. Tang L, Han B, Persson K, Friesen C, He T, Sieradzki K, Ceder G (2010) Electrochemical stability of nanometer-scale Pt particles in acidic environments. J Am Chem Soc 132(2):596–600
65. Liu G, Zhang H, Zhai Y, Zhang Y, Xu D, Z-g S (2007) Pt_4ZrO_2/C cathode catalyst for improved durability in high temperature PEMFC based on H_3PO_4 doped PBI. Electrochem Commun 9(1):135–141
66. Landsman DA, Luczak FJ (2003) In: Vielstich W, Lamm A, Gasteiger H (eds) Handbook of fuel cells – fundamentals, technology and applications, vol 4. Wiley, Chicester, pp 811–831
67. Neyerlin KC, Singh A, Chu D (2008) Kinetic characterization of a Pt-Ni/C catalyst with a phosphoric acid doped PBI membrane in a proton exchange membrane fuel cell. J Power Sources 176(1):112–117
68. Schmidt TJ, Baurmeister J (2008) Properties of high-temperature PEFC Celtec-P 1000 MEAs in start/stop operation mode. J Power Sources 176(2):428–434
69. Luczak FJ, Landsman DA (1984) Ordered ternary fuel cell catalysts containing platinum, cobalt and chromium. US Patent 4,447,506
70. Luczak FJ, Landsman DA (1987) Ordered ternary fuel cell catalysts containing platinum and cobalt and method for making the catalyst. US Patent 4,677,092
71. Beard B, Ross PN Jr (1990) The structure and activity of platinum-cobalt alloys as oxygen reduction electrocatalysts. J Electrochem Soc 137(11):3368–3374
72. Glass JT, Cahen GL, Stoner GE (1987) The effect of metallurgical variables on the electrocatalytic properties of platinum-chromium alloys. J Electrochem Soc 134(1):58–65
73. Mukerjee S, Srinivasan S (1993) Enhanced electrocatalysis of oxygen reduction on platinum alloys in proton exchange membrane fuel cells. J Electroanal Chem 357(1–2):201–224
74. Mukerjee S, Srinivasan S, Soriaga MP (1995) Role of structural and electronic properties of Pt and Pt alloys on electrocatalysis of oxygen reduction. An in situ XANES and EXAFS investigation. J Electrochem Soc 142(5):1409–1422
75. Paulus UA, Scherer GG, Wokaun A, Schmidt TJ, Stamenkovic V, Radmilovic V, Markovic NM, Ross PN (2001) Oxygen reduction on carbon-supported Pt-Ni and Pt-Co alloy catalysts. J Phys Chem B 106(16):4181–4191
76. Stamenkovic V, Fowler B, Mun BS, Wang B, Ross PN, Lucas CA, Markovic NM (2007) Improved oxygen reduction activity on Pt3Ni(111) via increased surface site availability. Science 315(5811):493–497
77. Stamenkovic V, Schmidt TJ, Ross PN, Markovic NM (2002) Surface composition effects in electrocatalysis: kinetics of oxygen reduction on well-defined Pt3Ni and Pt3Co alloy surfaces. J Phys Chem B 106(46):11970–11979
78. Parrondo J, Mijangos F, Rambabu B (2010) Platinum/tin oxide/carbon cathode catalyst for high temperature PEM fuel cell. J Power Sources 195(13):3977–3983
79. Qian G (2008) Fluorine-containing polybenzimidazoles for high temperature polymer electrolyte membrane fuel cell applications. Ph.D. thesis, Rensselaer Polytechnic Institute, Troy
80. Gasteiger H, Markovic NM (2009) Just a dream – or future reality? Science 324(5923):48–49
81. Debe MK, Schmoeckel AK, Vernstrom GD, Atanasoski R (2006) High voltage stability of nanostructured thin film catalysts for PEM fuel cells. J Power Sources 161(2):1002–1011
82. Strasser P (2009) Dealloyed Pt bimetallic electrocatalysts for oxygen reduction. In: Vielstich W, Yokokawa H, Gasteiger HA (eds) Handbook of fuel cells: advances in electrocatalysis, materials, diagnostics, and durability. Wiley, New York, pp 30–47
83. Lefevre M, Proietti E, Jaouen F, Dodelet J-P (2009) Iron-based catalysts with improved oxygen reduction activity in polymer electrolyte fuel cells. Science 324(5923):71–74
84. MCFC and PAFC R&D Workshop Summary Report. US Department of Energy (2010) http://www1.eere.

energy.gov/hydrogenandfuelcells/pdfs/mcfc_pafc_workshop_summary.pdf
85. Hu Y, Jensen JO, Zhang W, Martin S, Chenitz R, Pan C, Xing W, Bjerrum NJ, Li Q (2015) Fe3C-based oxygen reduction catalysts: synthesis, hollow spherical structures and applications in fuel cells. J Mater Chem A 3(4):1752–1760. https://doi.org/10.1039/C4TA03986F
86. Singdeo D, Dey T, Gaikwad S, Andreasen SJ, Ghosh PC (2017) A new modified-serpentine flow field for application in high temperature polymer electrolyte fuel cell. Appl Energy 195:13–22. https://doi.org/10.1016/j.apenergy.2017.03.022
87. Yu S, Xiao L, Benicewicz BC (2008) Durability studies of PBI-based high temperature PEMFC. Fuel Cells 8(3–4):165–174
88. Okae I, Kato S, Seya A, Kamoshita T (1990) Study of the phosphoric acid management in PAFCs. In: The chemical society of Japan 67th spring meeting, p 148
89. Manufacturing for the Hydrogen Economy: Manufacturing Research and Development of PEM Fuel Cell Systems for Transportation Application (2005) U.S. Department of Energy. http://www1.eere.energy.gov/hydrogenandfuelcells/pdfs/mfg_wkshp_fuelcell.pdf
90. Hydrogen Fuel Cell Vehicle and Station Deployment Plan: A Strategy for Meeting the Challenge Ahead (2009) California Fuel Cell Partnership. http://www.fuelcellpartnership.org/
91. Feitelberg AS, Stathopoulos J, Qi Z, Smith C, Elter JF (2005) Reliability of plug power GenSys fuel cell systems. J Power Sources 147(1–2):203–207
92. Schmidt TJ, Baurmeister J (2006) Durability and reliability in high temperature reformed hydrogen PEFCs. ECS Trans 3(1):861–869
93. Mocoteguy P, Ludwig B, Scholta J, Nedellec Y, Jones DJ, Roziere J (2010) Long-term testing in dynamic mode of HT-PEMFC H3PO4/PBI celtec-P based membrane electrode assemblies for Micro-CHP applications. Fuel Cells 10(2):299–311
94. Mocoteguy P, Ludwig B, Scholta J, Barrera R, Ginocchio S (2009) Long term testing in continuous mode of HT-PEMFC based H3PO4/PBI celtec-P MEAs for u-CHP applications. Fuel Cells 9(4):325–348
95. Garsany Y, Gould BD, Baturina OA, Swider-Lyons KE (2009) Comparison of the sulfur poisoning of PBI and nafion PEMFC cathodes. Electrochem Solid-State Lett 12(9):B138–B140
96. Schmidt TJ, Baurmeister J (2008) Development status of PBI based high-temperature membrane electrode assemblies. ECS Trans 16(2):263–270
97. Reiser CA, Bregoli L, Patterson TW, Yi JS, Yang JD, Perry ML, Jarvi TD (2005) A reverse-current decay mechanism for fuel cells. Electrochem Sol Let 8(6):A273–A276
98. Puffer RH Jr, Hoppes GH (2004) Development of a flecible pilot high temperature MEA manufacturing line. Fuel Cell Sci Eng Technol:573–579
99. Puffer RH Jr, Rock SJ (2009) Recent advances in high temperature proton exchange membrane fuel cell manufacturing. J Fuel Cell Sci Tech 6(4):041013/041011–041013/041017
100. Harris TAL, Walczyk D (2006) Development of a casting technique for membrane material used in high-temperature PEM fuel cells. J Manuf Process 8(1):19–31
101. Reduction of greenhouse gas emissions through fuel cell combined heat and power applications (2008) www.fuelcells.org/info/residentialsavings.pdf. Accessed 15–19 June 2008
102. Schmidtz R (2009) Japan working toward fuel-cell reality. Marketplace, December 8, p 1
103. Celtec MEAs: Membrane Electrode Assemblies for High Temperature PEM Fuel Cells (2010) BASF Fuel Cell GmbH. http://www.basf-fuelcell.com/en/projects/celtec-mea.html
104. Celtec® MEAs: Membrane Electrode Assemblies for High Temperature PEM Fuel Cells BASF. http://www.basf-fuelcell.com/cm/internet/Fuel_Cell/en/function/conversions:/publish/content/Microsite/Fuel_Cell/2474_Flyer_Celtec_P_Mea_ak3_jk.pdf
105. High-Temperature Fuel Cell System for Residential Applications (2009) Plug Power. http://www.plugpower.com/products/residentialgensys/residentialgensys.aspx
106. Serenus 166/390 Air C v2.5 (2010) Serenergy. http://www.serenergy.com/files/assets/documentation/166_390%20Air%20C%20v2.5%20data%20sheet_v1.1-0210.pdf
107. ClearEdge Power, Delivering Smart Energy Today. (2009) http://www.clearedgepower.com/. June 2010
108. Delventhal S (2017) What's ahead for the fuel-cell industry in 2017. Investopedia. http://www.investopedia.com/news/whats-ahead-fuelcell-industry-2017/
109. Emissions of Greenhouse Gases Report (2009) U.S. Energy Information Administration. http://www.eia.doe.gov/oiaf/1605/ggrpt/#ercde
110. Why 100 Hydrogen Stations: A California Fuel Cell Parntership White Paper (2017) California Fuel Cell Partnership. https://cafcp.org/sites/default/files/100-Stations-White-Paper-for-Public.pdf
111. A California Road Map: The Commercialization of Hydrogen Fuel Cell Vehicles (2014). https://cafcp.org/sites/default/files/Roadmap-Progress-Report2014-FINAL.pdf
112. SunHydro: Solar Powered Hydrogen Fueling Stations. (2017) SunHydro. http://www.sunhydro.com/locations/
113. Driving VW's fuel-cell prototypes (2008) Telegraph Media Group Limited. http://www.telegraph.co.uk/motoring/green-motoring/3520714/Driving-VWs-fuel-cell-prototypes.html
114. Innovative Danish technology uses methanol to make fuel cell vehicles competitive (2009, December) http://www.renewableenergyfocus.com/view/5650/

innovative-danish-technology-uses-methanol-to-make-fuel-cell-vehicles-competitive/
115. DLR Motor Glider Antares Takes Off in Hamburg – Powered by a Fuel Cell (2009) German Aerospace Center. http://www.dlr.de/en/desktopdefault.aspx/tabid-13/135_read-18278/
116. What's Next after the Dreamliner? Think Fuel Cells (2009, September 18) http://www.designnews.com/article/354516-What_s_Next_after_the_Dreamliner_Think_Fuel_Cells.php
117. UltraCell XX25: Mobile Power for Mobile Applications (2008) Ultracell. http://www.ultracellpower.com/assets/XX25_Data_Sheet_01-22-2009.pdf
118. UltraCell XX55: Extreme Mobile Power for Demanding Applications (2008) Ultracell. http://www.ultracellpower.com/assets/XX55_Data_Sheet_01-27-2009.pdf
119. Serenus Methanol fuel cell module – 350W (2010) Serenergy. http://www.serenergy.com/files/assets/documentation/Serenus%20H3%20E-350_datasheet_v1.1-0210.pdf
120. Methanol Power System: H_3 2500/3500 SerEnergy. http://serenergy.com/wp-content/uploads/2016/10/H3-2500-5000-48V_datasheet_v2.0-0916.pdf. Accessed 2017
121. Maget HJR (1970) Process for gas purification. US Patent 3,489,670, January 13.
122. McElroy JF (1989) SPE regenerative hydrogen/oxygen fuel cells for extraterrestrial surface applications. In: Energy conversion engineering conference, Washington, DC, August. Proceedings of the 24th intersociety. IEEE, pp 1631–1636
123. Rohland B, Eberle K, Strobel R, Scholta J, Garche J (1998) Electrochemical hydrogen compressor. Electrochem Acta 43(24):3841
124. Perry KA, Eisman GA, Benicewicz BC (2008) Electrochemical hydrogen pumping using a high-temperature polybenzimidazole (PBI) membrane. J Power Sources 177(2):478–484
125. Weidner JW (2016) Electrolyzer performance for producing hydrogen via a solar-driven hybrid-sulfur process. J Appl Electrochem 46(8):829–839. https://doi.org/10.1007/s10800-016-0962-0
126. Garrick TR, Gulledge A, Staser JA, Benicewicz B, Weidner JW (2015) Polybenzimidazole membranes for hydrogen production in the hybrid sulfur electrolyzer. ECS Trans 66(3):31–40. https://doi.org/10.1149/06603.0031ecst